Current Research (2017) Newfoundland and Labrador Department of Natural Resources
Geological Survey, Report 17-1, pages 147-168

GEOLOGY AND GEOCHEMISTRY OF THE SOKOMAN FORMATION IN THE GABBRO LAKE AREA, EASTERN LABRADOR TROUGH

J. Conliffe
Mineral Deposits Section

ABSTRACT

The Gabbro Lake area is situated in the southeastern portion of the Labrador Trough (NTS map area 23H/11), close to the boundary of the Churchill and Grenville provinces. Previous geological mapping in the area has been hampered by poor outcrop, coupled with a complex structural and metamorphic history. This study presents data from detailed re-logging of exploration drillcore, combined with petrographic analysis (including SEM–MLA) and whole-rock geochemical data, which provide new insights into the depositional history of the Sokoman Formation in the Gabbro Lake area.

The Sokoman Formation in the study area has four main facies: magnetite-rich banded iron formation (MBIF); magnetite-bearing mudstones (MM); hematite-rich granular iron formation (HGIF); and non-magnetic iron-rich siltstones and shales at the base of the Sokoman Formation. The Sokoman Formation also contains numerous interbedded tuffaceous units, which have been subdivided into Fe-rich and Ca-rich units, based on their petrographic and geochemical characteristics. The MBIF and MM are the main oxide-bearing facies in the Sokoman Formation, with HGIF restricted to thin (<5 m) intervals near the top of the formation. In contrast to the Sokoman Formation on the western margin of the Labrador Trough, which is predominantly composed of granular iron formation interpreted to have been deposited in a nearshore environment, the MBIF and MM in the Gabbro Lake area were likely deposited as chemical muds in deeper waters below the storm wave base, in either an outer shelf or slope-break setting. The Sokoman Formation in the Gabbro Lake area is underlain by sandstones, conglomerates, breccias and graphitic mudstones, which are interpreted as deep-water equivalents of the Wishart Formation, and were previously unrecognized in the southeastern Labrador Trough.

Geochemical analysis show that the MBIF and MM from the Gabbro Lake area have higher concentrations of Al_2O_3, K_2O, TiO_2, P_2O_5, LREE and selected trace elements compared with the HGIF and with data from the Sokoman Formation in the western part of the Labrador Trough. Petrographic studies and geochemical comparisons of tuffaceous units indicate that these higher concentrations are due to an input of volcaniclastic detritus during the deposition of the iron formation. There are possibly multiple sources of this volcaniclastic material, with the Fe-rich tuffaceous units likely being related to the Nimish Formation volcanic rocks to the north, and the Ca-rich tuffaceous units derived from an unknown volcanic centre located to the south or east.

INTRODUCTION

The Kaniapiskau Supergroup, in the Labrador Trough, is composed of a sequence of Paleoproterozoic sedimentary and volcanic rocks that were deposited in a continental basin at the margin of the Superior Craton (Wardle and Bailey, 1981; Le Gallais and Lavoie, 1982; Clark and Wares, 2005). The stratigraphy of the Kaniapiskau Supergroup is well defined and described from the central and northern Labrador Trough (Clark and Wares, 2005). The supergroup includes the Sokoman Formation iron formation, which is host to numerous economically important iron-ore deposits, and numerous studies have focused on the stratigraphy and geochemistry of the Sokoman Formation, particularly in the Schefferville and Menihek area (Zajac, 1974; Klein and Bricker, 1977; Klein and Fink, 1976; Fryer, 1977; Pufahl *et al.*, 2014). The results of the earlier work have shown that the Sokoman Formation occurring on the western margin of the Labrador Trough is a granular iron formation that was deposited on the continental margin in a high-energy, shallow-water, environment (Pufahl *et al.*, 2014).

The stratigraphy on the southeastern margin of the Labrador Trough is less well understood because of poor outcrop, less intense exploration activity and a complex post-depositional history, involving deformation and metamorphism associated with the Hudsonian and Grenville orogenies (Rivers, 1982). Correlations between stratigraphic units within the Kaniapiskau Supergroup from the western and eastern margins of the Labrador Trough are based on regional-scale government mapping (Wardle, 1979a, b; Ware and Wardle, 1979; Rivers, 1982). Prior to the current study, there have been no detailed stratigraphic or geochemical studies of the Sokoman Formation in the Gabbro Lake area.

In 2014, the Geological Survey of Newfoundland and Labrador undertook the task of re-logging select company drillholes from the Gabbro Lake area (NTS 23H/11; Figures 1 and 2). A number of samples from representative rock types in the Sokoman Formation were collected for whole-rock geochemical analysis. This report presents the results of this study, with the objective of determining the stratigraphic and sedimentological setting of the Kaniapiskau Supergroup in the southeastern Labrador Trough, with particular focus on the Sokoman Formation. The economic implications of these data will also be discussed.

PREVIOUS WORK AND HISTORY OF EXPLORATION

The first regional-scale geological maps of the Gabbro Lake area were produced by Labrador Mining and Explo-

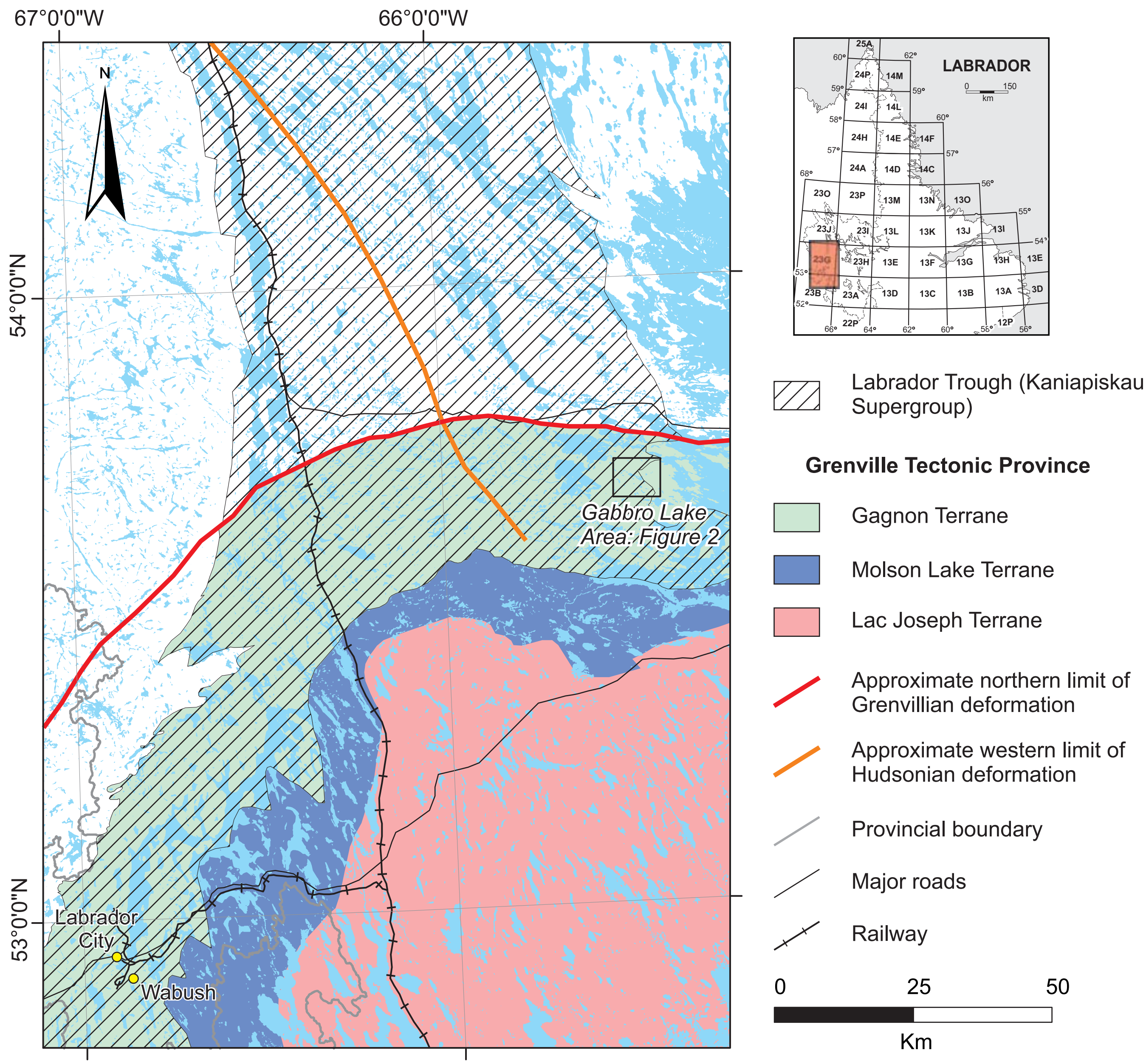

Figure 1. *Regional map showing location of the Gabbro Lake area, outline of the Labrador Trough and geological terranes in the Grenville Tectonic Province.*

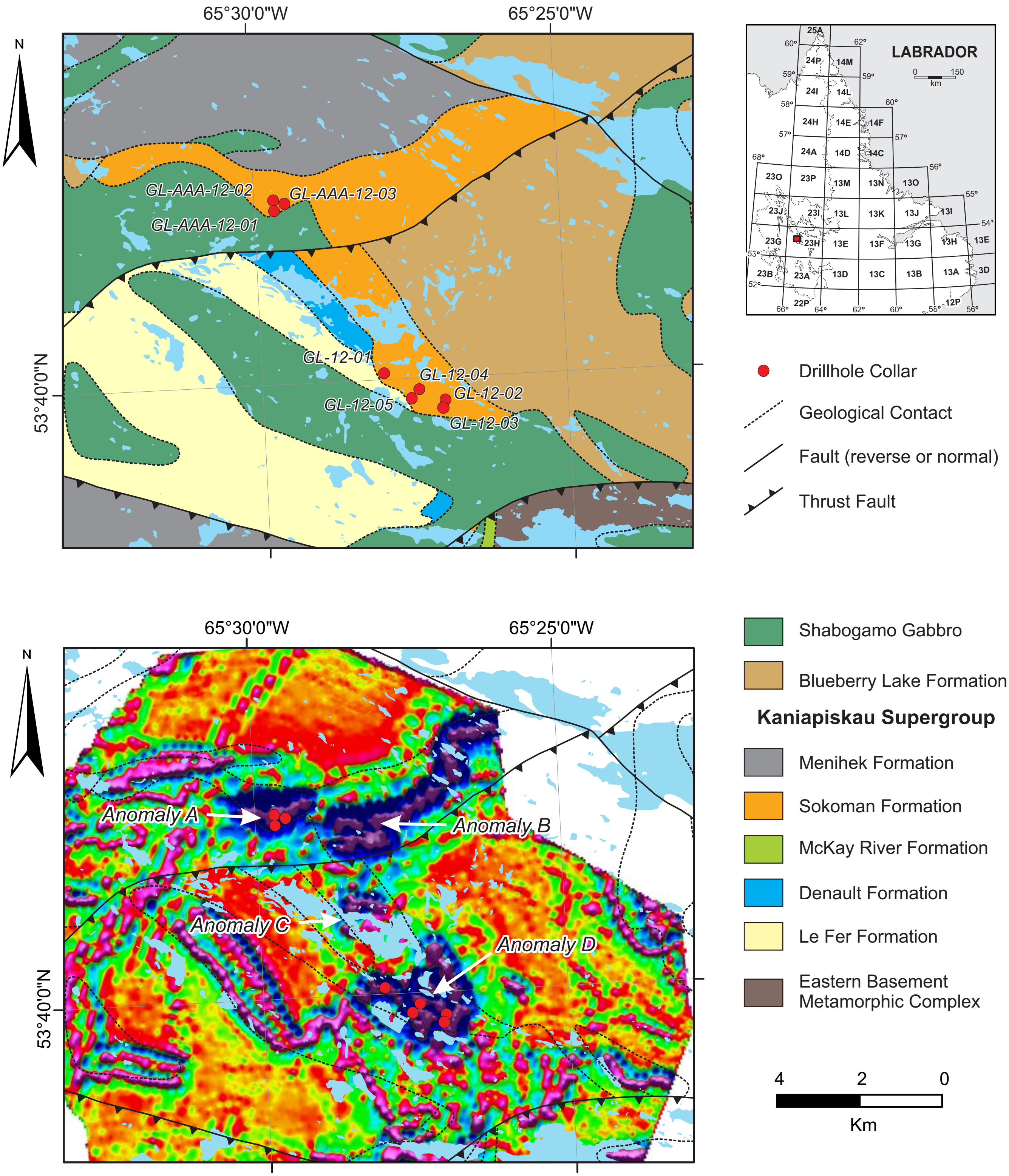

Figure 2. *Detailed geological map of the Gabbro Lake area (after Wardle* et al.*, 1985 and James, 1995) and airborne magnetics (second vertical derivative) from the Gabbro Lake area (adapted from Reid* et al.*, 2009). Also included are drillhole locations, and locations of aeromagnetic anomalies (from Froude and Fraser, 2012, 2013).*

ration Company Limited (LM&E) and the Iron Ore Company of Canada (IOC) in the late 1940s (Baird, 1950; Beland, 1950). Following on from this initial work, IOC geologists carried out detailed mapping focusing on the potential for economic ore deposits in the area, particularly iron-ore deposits (Tiphane, 1951; Peach, 1952; Slipp, 1952). Although the potential for significant high-grade (>60% Fe) iron-ore deposits in the area was deemed to be low, sporadic exploration activity by LM&E targeting base metals and other commodities continued up to the 1980s (Breau, 1957; Grant, 1980).

The Geological Survey of Canada mapped the western half of NTS map sheet 23H, which is summarized in a 1 inch to 4 miles scale map with accompanying notes describing the major rock units (Wynne-Edwards, 1961). This was followed by a multi-year mapping program as part of the Canada/Newfoundland Mineral Development Subsidiary Agreement (1977-1982), which led to the publication of a 1:100 000 scale map of the Gabbro Lake area by Wardle *et al.* (1985), as well as a series of government and academic publications describing the stratigraphy, structural, and metamorphic histories of the area (Wardle, 1979a; Noel and Rivers, 1980; Rivers, 1982; Brown, 1990; Noel, 1992). Further 1:50 000 mapping by James (1995) focused on the Blueberry Lake Group to the east of the study area, with compilation and reinterpretation of earlier mapping of the Knob Lake Group by Wardle *et al.* (1985).

In 2007, Metals Creek Resources and Golden Dory staked the Iron Horse Property in the Gabbro Lake area. Airborne geophysical surveys carried out in 2008 identified a number of magnetic, EM and radiometric anomalies (Reid *et al.*, 2009). These anomalies were subsequently determined to be associated with four separate lenses of highly magnetic iron formation, with strike lengths of 1.2 to 4 km and interpreted thicknesses of up to 500 m, which were called Anomaly A, B, C and D (Figure 2). A prospecting and sampling program on three of these anomalies in 2011 confirmed the presence of magnetic iron formation, with grab samples from outcrop and angular float assaying up to 52.7% Fe (Froude and Fraser, 2012). In 2012, Golden Dory completed two phases of diamond drilling, targeting two of these anomalies, with a total of 8 diamond-drill holes completed (three at Anomaly A, five at Anomaly D). Highlights from this drilling include 354.18 m of iron formation in drillhole GLAA-12-02 (at Anomaly A), grading 27.75% Fe, and 125.17 m of iron formation in drillhole GL-02-05 (at Anomaly D) grading 28.28% Fe (Froude and Fraser, 2012).

REGIONAL GEOLOGY

The Gabbro Lake area is located on the southeastern edge of the Labrador Trough, in the Gagnon Terrane of the Grenville Tectonic Zone (Figure 1). The Gagnon Terrane is a parautochthonous fold and thrust belt, bound to the north by the Grenville Front (northern limit of deformation associated with the Grenville Orogeny) and to the south by the Molson Lake Terrane (Figure 1). In the Gabbro Lake area, the Gagnon Terrane is composed of reworked Archean basement rocks, Paleoproterozoic sedimentary and volcanic rocks of the Kaniapiskau Supergroup and Blueberry Lake Group, and intrusive rocks of the Shabogamo Gabbro (Wardle, 1979a; Rivers, 1982; James and Connelly, 1995).

The Archean basement rocks form part of the Eastern Basement Metamorphic Complex, a sequence of granitoid gneisses and migmatites of unknown affinity that may possibly represent reworked parts of the Superior Craton (James and Connelly, 1995). The Kaniapiskau Supergroup lies unconformably on these basement rocks and was deposited on the eastern margin of the Superior Craton during the Paleoproterozoic (2.17 to 1.87 Ga; Rohon *et al.*, 1993; Findlay *et al.*, 1995; Machado *et al.*, 1997). The Kaniapiskau Supergroup can be correlated for over 1100 km along strike throughout the Labrador Trough, and its stratigraphy is best described from the central and northern parts of the Labrador Trough (Zajac, 1974; Wardle and Bailey, 1981; Le Gallais and Lavoie, 1982; Clark and Wares, 2005), where it is subdivided into three sedimentary and volcanic cycles (Figure 3; Wardle and Bailey, 1981; Clark and Wares, 2005). The base of the first cycle (Cycle 1) is composed of immature sandstones and siltstones associated with rifting of the Superior Craton (Seaward Group), which grade upward into passive margin sediments of the Swampy Bay and Attikamagen groups, including the Le Fer Formation (siltstone and shale), Denault Formation (dolomite), Fleming Formation (chert breccia) and Dolly Formation (shale and siltstone) (Clark and Wares, 2005). Cycle 2 is a transgressive sequence that progresses from shelf-type rocks of the Wishart Formation (sandstone and siltstones) and the Sokoman Formation (iron formation) at the base to deeper water turbidites of the Menihek Formation at the top. The intermediate to mafic volcanic and volcaniclastic rocks of the Nimish Formation are interbedded with the Sokoman Formation in the Dyke Lake area (Evans, 1978). Locally, Cycle 2 rocks are unconformably overlain by the Tamarack River Formation arkosic sandstones and siltstones (Cycle 3), which are interpreted as a synorogenic molasse.

Geological mapping in the southeastern Labrador Trough indicates that Kaniapiskau Supergroup sediments associated with rifting of the Superior continent (Seaward Group) are absent, where the oldest unit identified in the area is composed of the Le Fer Formation sandstones and siltstones (Wardle, 1979a; Rivers, 1982). Overlying the Le Fer Formation, most other formations of the Kaniapiskau Supergroup, as defined to the west, have been recorded,

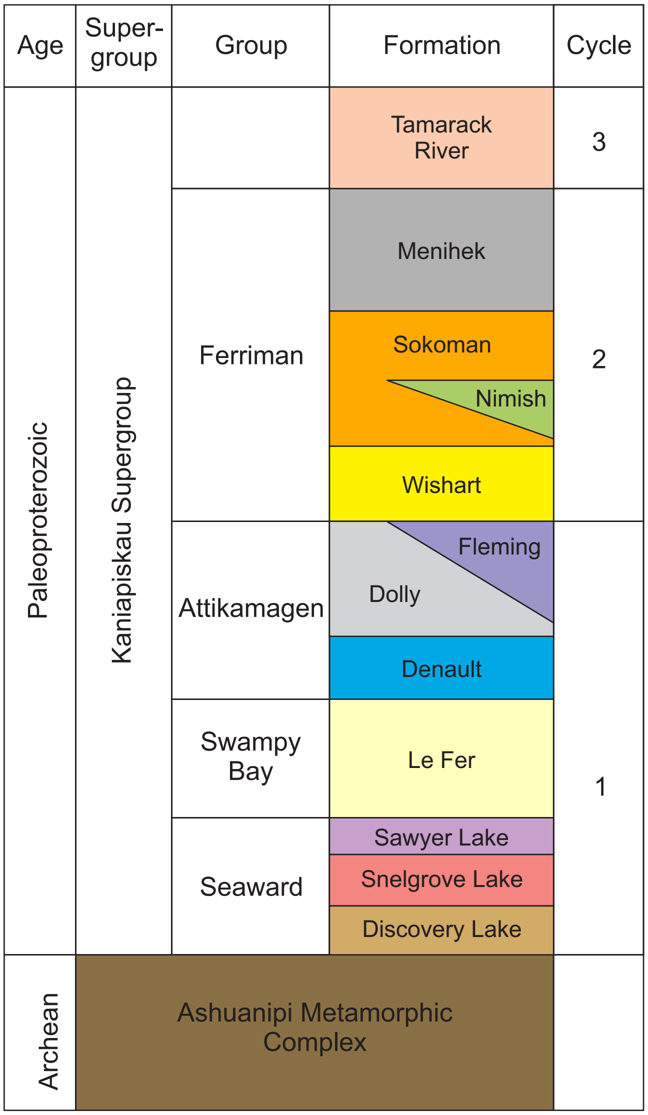

Figure 3. *Simplified stratigraphy of the Kaniapiskau Supergroup.*

with the exception of the Fleming Formation and the quartzites of the Wishart Formation (Rivers, 1982). In addition, a number of mafic to ultramafic volcanic and tuffaceous units occur that are unique to this area (Rivers, 1982; Noel, 1992). Noel (1992) subdivided these volcanic rocks into three chemically distinct mafic volcanic sequences; two mafic to ultramafic sequences in tectonic contact with the Kaniapiskau Supergroup (McKay River and Rose Bay formations) and a suite of high-level basaltic dykes and tuffaceous rocks interbedded with the Sokoman and Denault formations (sub-eruptive suite). The sub-eruptive suite is chemically similar to the Nimish Formation (Noel, 1992), and may represent an early phase of explosive volcanism prior to the more voluminous magmatism recorded in the Dyke Lake area (>800 m of basalt; Evans, 1978). Alternatively, the tuffaceous units may record volcanic activity at a spreading centre some distance to the east of the study area (Noel, 1992).

In the southeastern Labrador Trough, the Kaniapiskau Supergroup is unconformably overlain by the Blueberry Lake Group (Wardle, 1979a; James and Connelly, 1995). The Blueberry Lake Group is composed of a basal conglomerate, overlain by a sequence of fine-grained clastic sedimentary rocks, felsic crystal and lithic tuffs, and less abundant rhyolite, and an andesitic to dacitic porphyry (James and Connelly, 1995). Felsic volcanic rocks from the Blueberry Lake Group have yielded a U–Pb zircon age 1652 ± 5 Ma (James and Connelly, 1995). This age indicates that the Blueberry Lake Group was deposited at the same time as the emplacement of the Trans Labrador batholith to the south (at ~1650 Ma; James, 1994), and it is interpreted to represent filling of a back-arc basin located to the north of a continental magmatic arc (James, 1994).

All the rock units in the Gagnon Terrane are intruded by the Shabogamo Gabbro, a medium- to coarse-grained olivine gabbro. Gower *et al.* (1990) correlated the Shabogamo Gabbro with the Michael Gabbro of eastern Labrador, and Emslie *et al.* (1997) demonstrated that the two suites had similar evolutionary histories involving subcontinental lithospheric mantle. The U–Pb age constraints from the Shabogamo Gabbro indicate emplacement at ~1450 Ma (Connelly and Heaman, 1993).

STRUCTURAL AND METAMORPHIC SETTING

The structural history of the Gabbro Lake area is complex, with overprinting effects of the Hudsonian Orogeny (1.82 to 1.77 Ga; Wardle *et al.*, 2002) and the Grenville Orogeny (*ca.* 1.09 to 0.98 Ga; Rivers *et al.*, 2012). The evidence for deformation related to the Hudsonian Orogeny is often difficult to ascertain, due to the paucity of outcrop and the overprinting effects of deformation associated with the later Grenvillian Orogeny (Rivers, 1982; Brown, 1990). However, Rivers (1982) identified a high-angle cleavage to the axial plane of folds, which he interpreted to represent a Hudsonian fold crosscut by cleavage associated by Grenvillian deformation. Brown (1990) also showed that many structural features in the area predate intrusion of the Shabogamo Gabbro (1450 Ma), and these pre-Grenvillian structures were also attributed to Hudsonian deformation. Where present, these Hudsonian structures define a series of southwest-verging, northeast-plunging fold nappes and associated thrusts (Ware and Wardle, 1979; Rivers, 1982; Brown, 1990).

Grenvillian deformation is characterized by a penetrative east–west structural grain (S1) and at least two, and possibly three, generations of folding (Rivers, 1982). Structural studies to the west of the Gabbro Lake area show that this deformation occurred during the development of a ductile, metamorphic fold and thrust belt at upper to middle crustal levels (Brown, 1990). Additionally, the Gabbro Lake area is separated into a number of different tectonic domains by large-scale, west- and northwest-trending thrusts, identified through interpretation of aeromagnetic data and observed variations in rock types (Rivers, 1982; Brown, 1990). These thrust faults are either Hudsonian or Grenvillian, and the reactivation of Hudsonian thrust faults during Grenvillian deformation is also considered likely (Rivers, 1982).

Metamorphic grades vary widely across the Gabbro Lake area, and are complicated by the overprinting of Hudsonian and Grenvillian metamorphism, as well as contact metamorphism associated with the intrusion of the Shabogamo Gabbro (Rivers, 1982). Mapping of the Kaniapiskau Supergroup north of the Grenville Front indicate that metamorphic grades are sub-greenschist to greenschist and increase from west to east (Ware and Wardle, 1979). It is likely that the Kaniapiskau Supergroup in the Gabbro Lake area attained a similar metamorphic grade prior to the Grenville Orogeny (Rivers, 1982). Prograde metamorphism associated with the Grenville Orogeny largely overprinted Hudsonian metamorphism, and increases from lower greenschist facies in the north to upper greenschist and lower amphibolite facies in the south (Rivers, 1982; Brown, 1990). Contact metamorphism associated with the intrusion of the Shabogamo Gabbro is recoded as hornsfels textures adjacent to the gabbro bodies (Rivers, 1982).

STRATIGRAPHY OF THE KANIAPISKAU SUPERGROUP

Previous interpretations of the stratigraphy of the Kaniapiskau Supergroup in the Gabbro Lake area were constrained by lack of outcrop or high-resolution geophysical surveys. Sparse outcrops of Sokoman Formation iron formation and Le Fer Formation schists and shales occur in the west of the area, with outcrops of the Blueberry Lake Group occurring in the east (Wardle *et al.*, 1985; James, 1995). There are also numerous outcrops of Shabogamo Gabbro, which form many of the more prominent topographic features (Rivers, 1982). However, no geological contacts were recorded, and the distribution of the main rock types, and the location of major faults, was based on interpretation of low-resolution regional aeromagnetic studies and aerial photographs (Rivers, 1982).

Recently obtained high-resolution aeromagnetic data has shown that the published geological maps of the region (Wardle *et al.*, 1985; James, 1995) need to be reinterpreted (Figure 2). The following stratigraphic descriptions are based on the re-logging of five diamond-drill holes from Anomaly D in the south of the area (Figures 2 and 4). These holes were selected as they provide a complete record of the stratigraphy between the Sokoman and the Le Fer formations, and hence facilitate correlations of the Kaniapiskau Supergroup in the Gabbro Lake area with units identified in the central and northern parts of the Labrador Trough (Zajac, 1974; Wardle and Bailey, 1981; Le Gallais and Lavoie, 1982; Clark and Wares, 2005).

SOKOMAN FORMATION

The Sokoman Formation iron formation has been the main target of mineral exploration, and has been intersected in all drillholes. The true thickness of the formation is unknown, as the upper contact has not been observed. Drilling recorded intersections of iron formation up to 140 m, but these have been structurally thickened, with evidence of fold thickening and repetition observed in all drillholes, and repetition by thrust faulting observed in drillhole GL-12-05.

The Sokoman Formation is subdivided into a number of primary facies, based on variations in textures, stratigraphic position and petrographic analyses of polished thin sections. Four samples were also analyzed using the combination of scanning electron microscopy (SEM) backscatter images and mineral liberation analysis (MLA) software at Memorial University of Newfoundland, following the procedure outlined in Sylvester (2012). The SEM-MLA approach allows the abundance of mineral species to be quantified, as well as determining the detailed textural relationships in fine-grained samples.

Magnetite-rich Banded Iron Formation (MBIF)

Magnetite-rich iron formation, with alternating iron-rich and silica-rich layers (Plate 1A) is the most common facies in the middle portion of the Sokoman Formation, and may be equivalent to the Middle Iron Formation described in the central Labrador Trough (Zajac, 1974; Wardle, 1979b). The layers range in thickness from <2 mm to >5 cm, and commonly show evidence of folding and small-scale faulting. The iron-rich layers consist of 20 to 60% fine-grained, subhedral magnetite having varying proportions of stilpnomelane, grunerite, Fe-carbonates, quartz and minor pyrite in some samples (Plate 2A). Fine-grained stilpnomelane is the most common Fe-silicate in lower metamorphic grades, and the proportion of medium- to coarse-grained grunerite increases as metamorphic grade increases, with euhedral garnets also recorded in highly metamorphosed samples (Plates 1B and 2B). Secondary magnetite is observed as overgrowths on coarse-grained grunerite and garnet (Plate 2C), indicating recrystallization of iron oxides during metamorphism. The silica-rich layers consist of (in

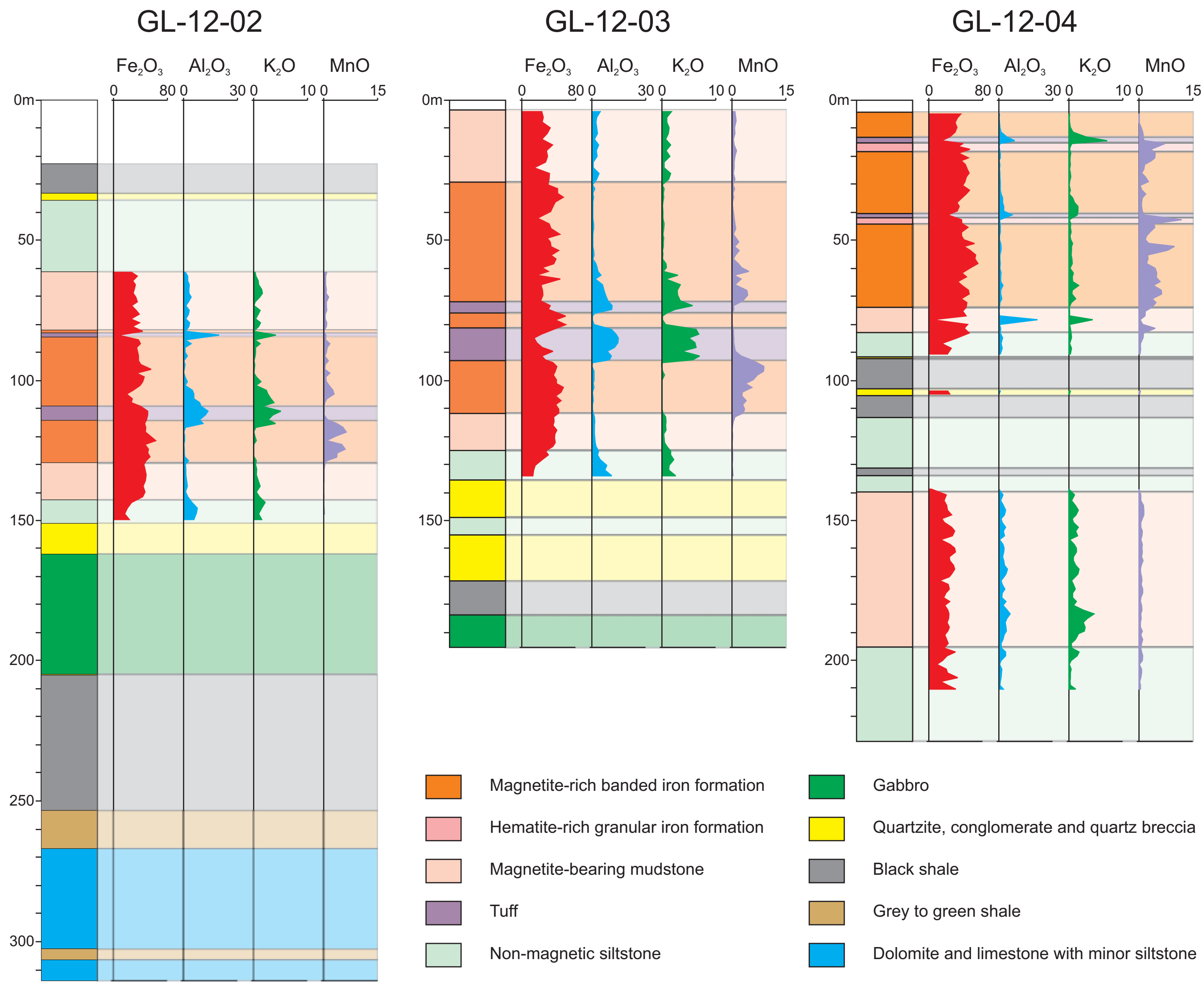

Figure 4. *Strip logs showing the results of detailed re-logging of three diamond-drill holes, as well as assay data from Froude and Fraser (2012).*

order of abundance) medium-grained quartz, carbonate (siderite and Mn-rich siderite) and magnetite, and fine-grained acicular grunerite also recorded in silica-rich layers that were exposed to higher metamorphic grades. SEM-MLA has also identified fine-grained ilmenite and apatite in metamorphosed MBIF samples.

The magnetite-rich iron formation is classified as a banded iron formation (BIF), based on the fine grain size and alternating iron-rich and silica-rich layers (Clout and Simonson; 2005).

Hematite-rich Granular Iron Formation (HGIF)

Hematite-rich iron formation is highly variable in texture, and recorded in the upper part of the Sokoman Formation in two of the five drillholes logged (GL-12-01 and GL-12-04). It lacks the regular mm- to cm-scale alternating layers of the magnetite-rich banded iron formation, and instead consists of irregular bands of iron-rich, silica-rich or mixed iron formation (generally >5 cm thick; Plate 1C). The mineralogy of the hematite-rich iron formation is also variable, and it is characterized by hematite as the main iron oxide present, although significant magnetite is also present in some layers. Iron-rich layers generally consist of hematite, quartz and carbonate, and minor magnetite, minnesotaite and chlorite. The iron-poor layers commonly contain rounded oolites that have delicate concentric hematite layers, and a quartz cement (Plate 2D) and minor Fe-silicates. Bands of pink rhodonite (Mn-silicate) are also recorded in the hematite-rich iron formation (Plate 1C).

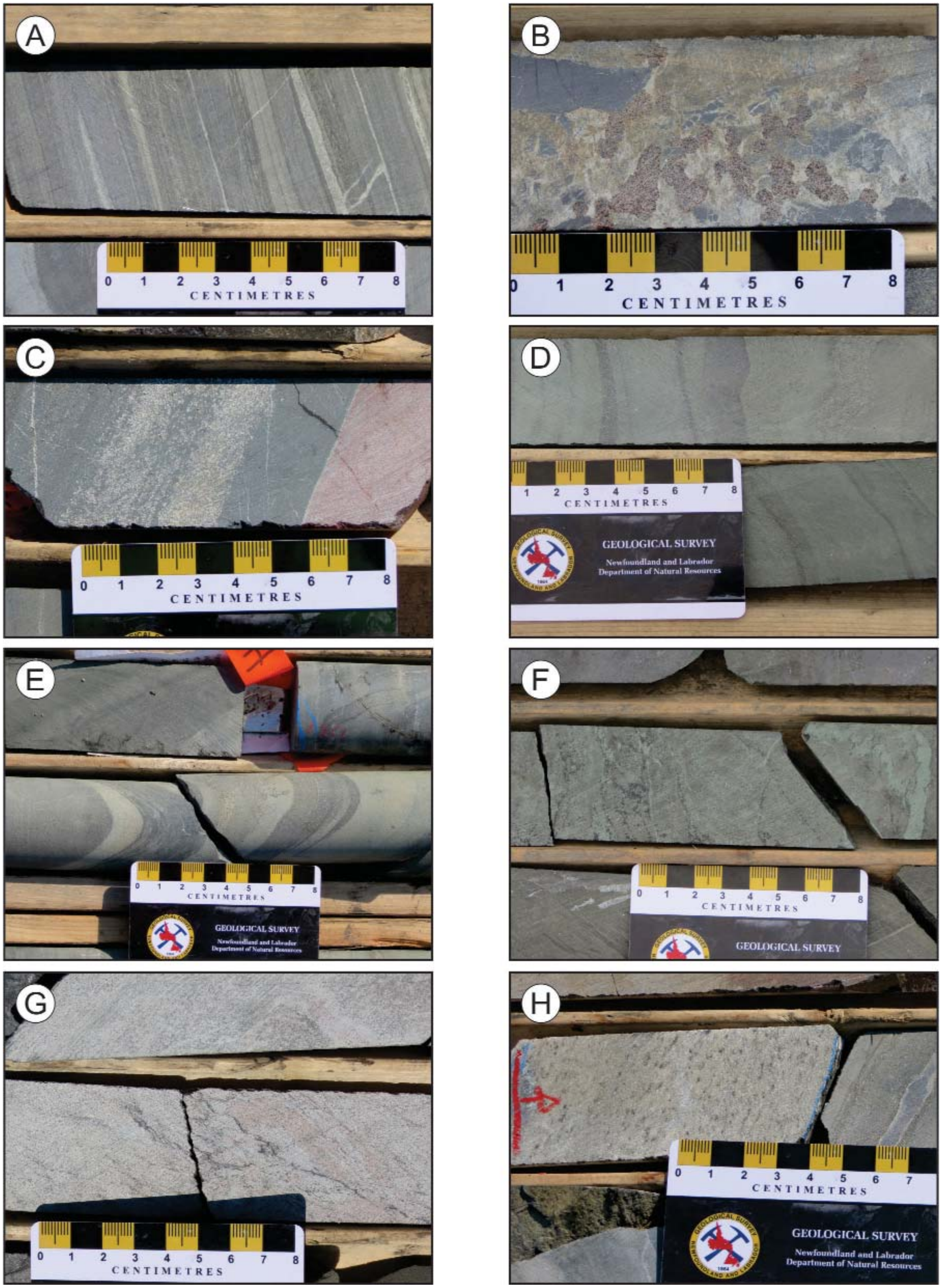

Plate 1. *A) MBIF with alternating iron-rich and silica-rich layers (GL-12-02; 136 m); B) Strongly metamorphosed MBIF, with large euhedral garnets and coarse grunerite (GL-12-03; 96.8 m); C) HGIF with hematite-rich layers and a layer of pink rhodonite (GL-12-04; 15.5 m); D) Fine-grained, green magnetite-bearing mudstone (GL-12-03; 18.6 m); E) Non-magnetic siltstone (GL-12-04; 113 m); F) Fe-rich tuffaceous unit with strong chlorite alteration (GL-12-03, 74.3 m); G) Ca-rich tuff (GL-12-02; 113 m); H) Ca-rich tuff (GL-12-04; 15.3 m).*

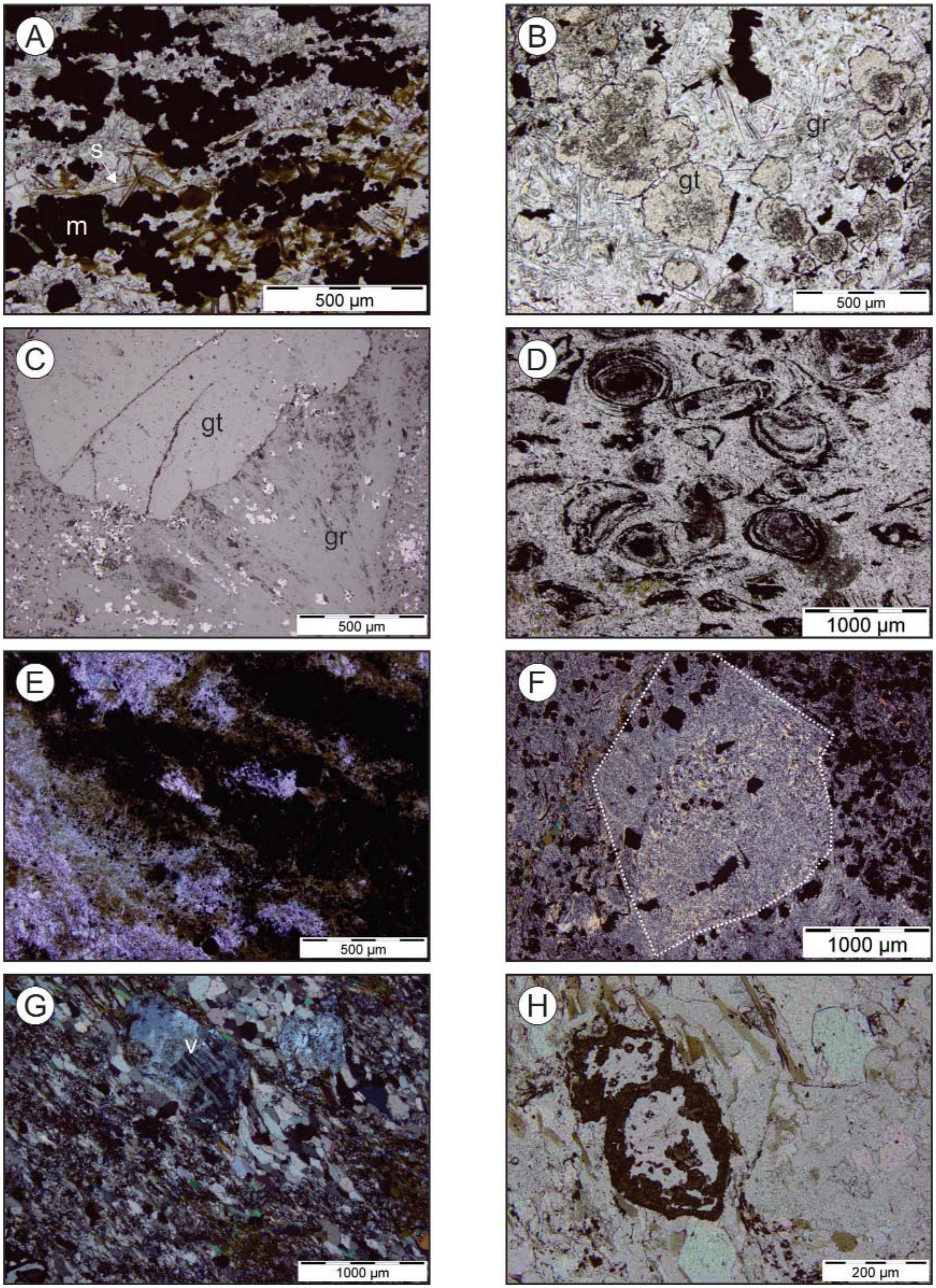

Plate 2. *A) Photomicrograph of iron-rich layer in MBIF, with euhedral magnetite and brown stilpnomelane (GL-12-02; 95.1 m); B) Metamorphosed MBIF, with garnet (gt) and grunerite (gr) (GL-12-03; 70.3 m); C) Reflected light photomicrograph of metamorphosed MBIF, with euhedral magnetite (white) overgrowing garnet (gt) and grunerite (gr) (GL-12-03; 70.3 m); D) HGIF with hematite oolites in quartz matrix (GL-12-01; 10.2 m); E) Fine-grained MM, with euhedral magnetite (black), stilpnomelane (brown) and diopside (white) (GL-12-05; 114.5 m); F) Fe-rich tuffaceous unit, with dashed line showing outline of possible pyroxene or olivine phenocryst replaced by chlorite (GL-12-05; 53.5 m); G) Volcaniclastic detritus (v) composed of feldspar in Ca-rich tuffaceous unit (GL-12-04; 15 m); H) Skeletal rutile around calcite fragment in Ca-rich tuffaceous unit (GL-12-04, 15 m).*

In contrast to the magnetite-rich banded iron formation, the hematite-rich iron formation is classified as a granular iron formation (GIF) based on its coarser grain size, presence of oolites, and irregular thicker layers (Clout and Simonson, 2005).

Magnetite-bearing Mudstone (MM)

Fine-grained, grey to green magnetic mudstones occur in the lower Sokoman Formation, and may be correlated with the Fe-oxide-poor Lower Iron Formation and Silicate Carbonate Iron Formation in the central part of the Labrador Trough (Zajac, 1974; Wardle, 1979b). The magnetic mudstone is finely laminated (<5 mm laminations; Plate 1D) and commonly calcareous. SEM-MLA and petrographic analyses indicate that these laminations consist of alternating layers composed of stilpnomelane, grunerite, euhedral to subhedral magnetite, siderite, ilmenite and apatite, and layers composed of diopside, calcite, ankerite, and grunerite (Plate 2E). Minor chlorite, biotite and albite were also identified by SEM-MLA.

Non-magnetic Siltstone

The lowermost magnetic mudstones of the Sokoman Formation grade into a non-magnetic, green, fine-grained siltstone (Plate 1E) having abundant iron carbonates and iron silicates but no iron oxides. Assay data indicate that this siltstone commonly contains >15% Fe when in close proximity to the contact with the Sokoman Formation (Froude and Fraser, 2012), and therefore it can be classified as an iron formation senso stricto (James, 1954). It may be correlated with the sequence of clastic silicate and carbonate rocks at the base of the Sokoman Formation in the central Labrador Trough (commonly referred to as the Ruth Formation; Zajac, 1974).

Tuffaceous Units

Numerous tuffaceous units are interbedded with the iron formation (Plate 1F, G, H), with individual units ranging in thickness from <5 cm to >1 m, and intervals of up to 12 m containing more than 50% tuffaceous units. Although metamorphism and alteration have resulted in the obliteration of many of the primary textures, normal grading has been locally preserved and recorded in some of these units. These fine- to medium-grained units are subdivided into two types based on their petrography and geochemistry (*see* below).

Fe-rich tuffaceous units are dark green to grey (Plate 1F), are typically altered and metamorphosed, and commonly display secondary chlorite veining. They are composed of euhedral magnetite and subrounded lithic fragments in a fine-grained matrix (chlorite and feldspar-rich). The lithic fragments are primarily composed of altered fine-grained chlorite, possibly representing a retrograde alteration of a mafic phase such as olivine or clinopyroxene (Plate 2F), and as rare orthoclase crystals. Ca-rich tuffaceous units are less common than the Fe-rich variety, and are restricted to thin (<50 cm) units. They range from beige to dark grey (Plate 1G, H). SEM-MLA and petrographic analysis of a carbonate-rich tuffaceous unit was recorded on a sample from drillhole GL-12-04 (Plate 1H), and illustrates a matrix of calcite (>50%), K-feldspar and biotite (Plate 2G), containing numerous detrital fragments. These detrital fragments are subangular to subrounded (up to 2 mm), and consist of K-feldspar, quartz, albite, apatite or fine-grained mixtures of these minerals. The albite is commonly altered and displays perthite textures (Plate 2G). Rutile and minor ilmenite are also observed. These minerals occur in the matrix where they are associated with K-feldspar and biotite, as well as in detrital fragments and surrounding grains of calcite and apatite where they form a distinct skeletal texture (Plate 2H).

WISHART FORMATION

The Wishart Formation has not been mapped or recognized in the Gabbro Lake area (Rivers, 1982). However, the quartzites, conglomerates and shales, that directly underlie the Sokoman Formation, are interpreted to represent equivalents of the massive crossbedded sandstones and siltstones, described as part of the Wishart Formation, from the western margin of the Labrador Trough (Simonson, 1984). The base of the Sokoman Formation is difficult to define, with thin (>50 cm) beds of quartzite, breccia and conglomerate (rounded quartz pebbles, Plate 3A) increasing in abundance toward the base of the formation. The upper 5 to 10 m of the Wishart Formation is dominated by massive quartzites (Plate 3B), breccia and conglomerates that grade into a thick (up to 75 m) sequence of black graphitic mudstone having common pyrite nodules (Plate 3C).

DOLLY FORMATION

The metasedimentary rocks underlying the Wishart Formation have only been recorded in one drillhole (GL-12-02). Here, the black mudstones at the base of the Wishart Formation have a sharp, lower contact with green siltstones and shales containing thin (<30 cm) sandstone beds (Plate 3D). This unit is interpreted to represent the Dolly Formation of the Attikamagen Group, which is recorded as occurring below the Wishart Formation north of the study area (Wardle, 1979b).

DENAULT FORMATION

The Denault Formation is a sequence of grey dolomitic marble (Plate 3E) having minor siltstone intervals. It has a

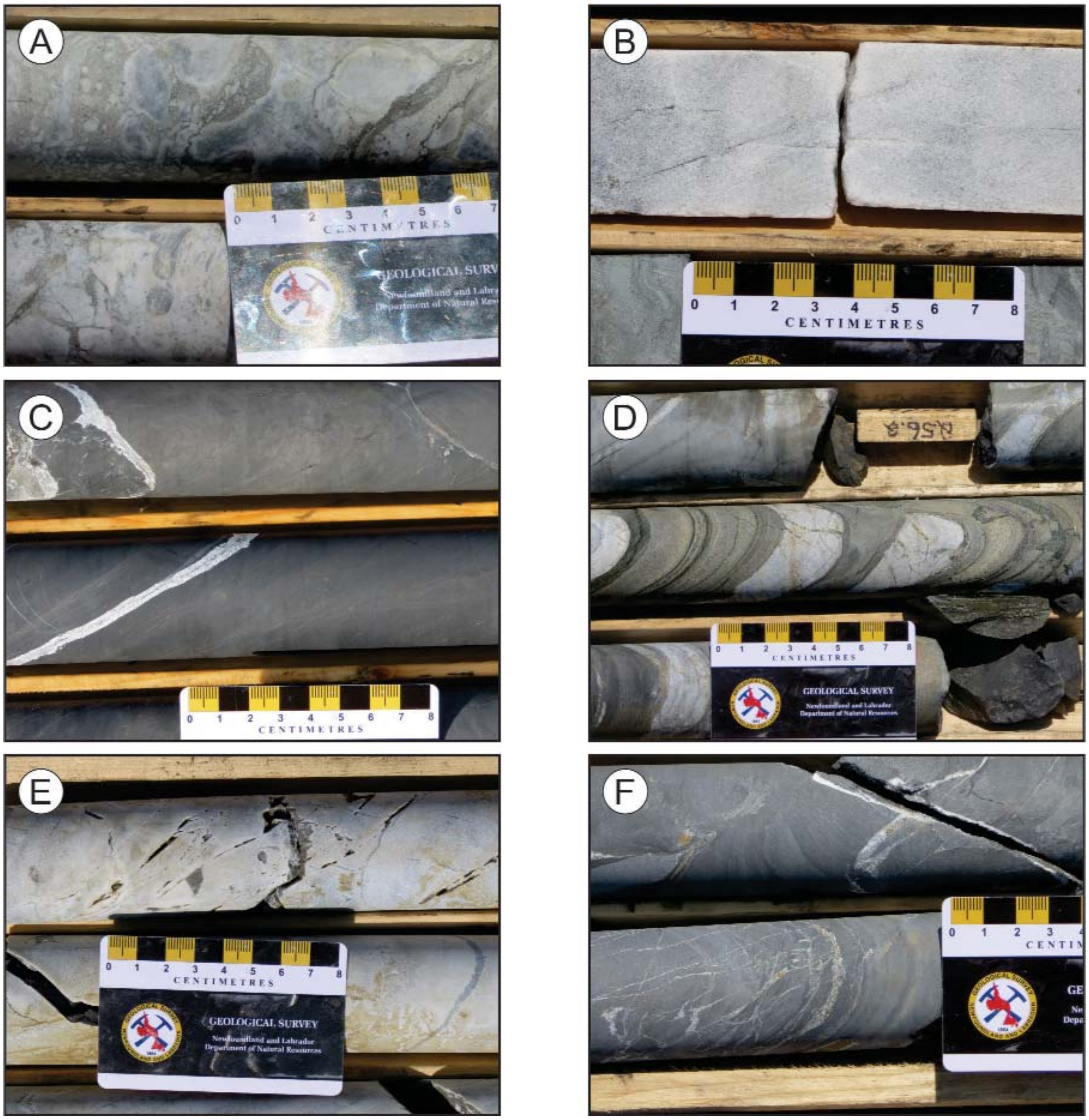

Plate 3. *A) Quartz conglomerate from top of Wishart Formation (GL-12-02; 153.9 m); B) Massive sandstone in Wishart Formation (GL-12-02; 151.7 m); C) Black, graphitic mudstone at base of Wishart Formation (GL-12-05; 180 m); D) Green siltstones and interbedded sandstones from the Dolly Formation (GL-12-02; 254.7 m); E) Metamorphosed dolomite of the Denault Formation (GL-12-02; 290 m); F) Black shales underlying Denault Formation, probable Attikamagen Formation (GL-12-02; 305.8 m).*

gradational upper and lower contact, and thin (<1 m) beds of dolomitic marble are recorded in the overlying and underlying units close to the contact. Some banding is present in the Denault Formation, but most primary textures have been destroyed by later metamorphism.

LE FER FORMATION

The Le Fer Formation is recorded at the base of drillhole GL-12-12, and consists of black to green siliceous mudstones (Plate 3F), minor graphitic intervals, abundant calcite veining and minor sulphides (pyrite and pyrrhotite).

SHABOGAMO GABBRO

Medium-grained, olivine-bearing gabbro has been recorded in three drillholes (GL-12-01, GL-12-02 and GL-12-03). This gabbro occurs as sills, and has been intersected through drilling over thicknesses from 0.5 to 20 m (not true thickness), and is located at the base of the Sokoman Formation and the top of the Wishart Formation. These gabbro sills represent the Shabogamo Gabbro, which forms many of the prominent ridges observed in the Gabbro Lake area (Rivers, 1982).

WHOLE-ROCK GEOCHEMISTRY

METHODS

Twenty-two samples of the Sokoman Formation were collected for detailed geochemical analysis. These included seven samples of magnetite-rich banded iron formation, three of hematite-rich granular iron formation, six of magnetic mudstone, and six from tuffaceous units.

All samples selected for geochemical analysis were prepared at the GSNL geochemistry laboratory in St. John's. Samples were milled using ceramic and tungsten carbide mills. Due to possible contamination from the tungsten carbide mill, tungsten and cobalt values are not reported. To determine precision and accuracy, reference standards and analytical duplicates were inserted at a frequency of one in twenty samples. Major-element compositions were analyzed by ICP-OES methods, following lithium tetraborate and metaborate fusion. Rare-earth elements (REE) and selected trace elements were determined by ICP-MS analysis following an identical sample digestion procedure, whereas the remaining trace elements (Be, Cu, Li, Mn, Ni, Pb, Rb, Sc, Ti, Zn) were analyzed by ICP-MS after total acid digestion. The loss-on-ignition (LOI) was calculated after heating the sample to 1000°C.

RESULTS

The major-element and trace-element compositions of samples from the Sokoman Formation are summarized in Tables 1 and 2. In addition, assay data from company reports (Froude and Fraser, 2012) were used to compile strip logs of selected drillholes (Figure 4). Geochemistry from the Sokoman Formation iron formation in the central Labrador Trough (referred to as AvSok-CT) was used for comparative purposes (data from Conliffe, 2016).

Magnetite-rich Banded Iron Formation (MBIF)

Fe_2O_3 and SiO_2 are the dominant major elements in all MBIF samples, with Fe_2O_3 + SiO_2 contents averaging 85.5 ± 7 wt. %, and Fe_2O_3 contents ranging from 32.6 to 55.8 wt. % (22.8 to 39 wt. % Fe). MnO values are highly variable, ranging from 0.1 to 8.5 wt. % (Figure 4). All other major-element contents are less than 5 wt. %. When compared with AvSok-CT, the MBIF in the study area has higher contents of CaO, Al_2O_3, TiO_2 and P_2O_5, and commonly K_2O (Figure 5).

The trace-element content of MBIF samples has been normalized to the average Sokoman Formation in the central Labrador Trough in order to determine relative contents of selected trace elements (Figure 6). This shows that the

Table 1. Summary statistics for major-element contents of MBIF, HGIF, MM and Fe-rich and Ca-rich tuffaceous units from the Gabbro Lake area. Also included are values for average Sokoman Formation in the central Labrador Trough (AvSok-CT)

	Magnetite-rich banded iron formation		Hematite-rich granular iron formation		magnetic mudstone		Fe-rich tuffaceous units		Ca-rich tuffaceous units		AvSok-CT	
n	7		3		6		3		3		8	
	Av.	Stdev.	Av.	Stdev.	Av.	Stdev.	Av.	Stdev.	Av.	Stdev.	Av.	Stdev.
SiO_2	40.6	7.7	42.3	13.4	41.0	5.6	32.5	13.5	29.5	2.1	44.0	4.3
Al_2O_3	1.3	0.5	0.2	0.0	3.2	1.4	14.1	3.0	8.8	2.7	0.1	0.0
Fe_2O_3	44.9	9.8	38.2	12.6	41.6	8.0	42.3	9.5	12.0	12.3	52.0	5.5
Fe	31.4	6.9	26.7	8.8	29.1	5.6	29.6	6.7	8.4	8.6	36.4	3.8
MgO	3.7	1.0	0.8	0.9	4.7	2.4	1.2	0.2	4.0	1.0	1.6	1.7
CaO	2.0	1.5	2.9	1.1	2.7	1.9	0.6	0.2	16.1	10.4	0.1	0.2
Na_2O	0.2	0.2	1.8	1.7	0.3	0.2	0.1	0.1	1.4	2.2	0.1	0.0
K_2O	0.5	0.3	0.1	0.1	1.5	0.8	4.3	1.4	4.4	2.7	0.1	0.0
TiO_2	0.32	0.23	0.04	0.01	0.53	0.76	0.82	0.28	3.92	1.71	0.00	0.00
MnO	2.4	3.0	10.3	4.9	0.4	0.2	0.8	0.7	4.3	1.2	0.4	0.5
P_2O_5	0.12	0.07	0.01	0.00	0.13	0.09	0.32	0.21	1.76	0.78	0.02	0.01
LOI	3.2	3.9	2.9	2.1	2.5	2.2	2.3	1.0	12.7	10.8	2.7	1.9
Total	99.2	0.8	99.5	0.8	98.7	0.6	99.3	1.2	98.9	0.5	100.0	0.8

MBIF has relatively higher contents of large ion lithophile elements (LILE) such as Rb, Sr and Ba. The transition metals (including V, Cr, Ni, Cu and Zn) have variable contents, with relatively high contents of Cr recorded in all but one sample (Figure 6). The Y content of MBIF is similar to AvSok-CT, but other high-field-strength elements (HFSE) show relatively increased contents (*e.g.*, Zr, Nb).

The total REE content (∑REE) of MBIF samples ranges from 48 to 86 ppm. In Figure 7, the REE data are normalized to the average value of Post-Archean Australian Shale (PAAS), and compared to REE data from the Sokoman Formation in the central Labrador Trough. This shows that MBIF samples have relatively higher contents of light rare-earth elements (LREE) compared to the samples from the central part of the Labrador Trough, with Pr/Yb_{PAASN} ratios of 1.19 to 1.67 (Figure 8). Five samples have positive Eu anomalies (Eu/Eu^*_{PAASN} of 1.32 to 1.66) and negligible Ce anomalies (Ce/Ce^*_{PAASN} of 0.89 to 1.08) and one sample has a negligible Eu anomaly (Eu/Eu^*_{PAASN} of 1.06) and a strong positive Ce anomaly (Ce/Ce^*_{PAASN} of 1.57).

Table 2. Summary statistics for trace-element and rare-earth-element contents of MBIF, HGIF, MM and Fe-rich and Ca-rich tuffaceous units for the Gabbro Lake area. Also included are values for average Sokoman Formation in the central Labrador Trough (AvSok-CT). $Eu/Eu^* = Eu_{PAASN}/((Sm_{PAASN}+Gd_{PAASN})/2)$. $Ce/Ce^* = Ce_{PAASN}/((La_{PAASN}+Pr_{PAASN})/2)$

	Magnetite-rich banded iron formation		Hematite-rich granular iron formation		magnetic mudstone		Fe-rich tuffaceous units		Ca-rich tuffaceous units		AvSoK-CT	
n	7		3		6		3		3		8	
	Av.	Stdev.	Av.	Stdev.	Av.	Stdev.	Av.	Stdev.	Av.	Stdev.	Av.	Stdev.
Rb	23	14	2	-	81	48	196	32	177	115	6	2
Sr	25	11	55	14	49	19	51	46	733	466	2	1
Ba	79	68	293	197	124	96	325	133	1233	207	12	18
V	45	29	11	3	50	53	189	110	125	108	15	4
Cr	47	41	4	2	125	224	67	6	137	65	2	1
Ni	56	27	36	7	94	121	44	8	30	10	31	4
Cu	9	4	3	1	26	46	58	87	5	4	5	1
Zn	43	16	38	24	50	22	65	29	121	16	26	8
Y	10	3	17	3	10	6	10	1	89	23	8	12
Zr	63	26	26	7	104	49	179	103	804	211	14	4
Nb	15	8	6	0	35	17	52	59	266	116	3	1
Ge	18	3	17	7	20	3	17	5	15	8	13	4
La	13.8	4.5	18.6	5.7	22.2	9.1	25.6	6.7	223.2	184.3	3.9	3.4
Ce	27.2	5.9	23.1	4.3	47.2	20.2	88.5	32.8	398.6	312.3	4.7	2.2
Pr	3.0	0.9	2.5	0.4	5.0	2.9	6.4	1.2	44.8	35.1	0.7	0.9
Nd	11.7	3.8	10.0	2.1	19.3	12.6	24.3	5.3	167.8	127.3	3.3	4.6
Sm	2.1	0.8	1.8	0.4	3.3	2.4	4.4	1.2	29.4	20.6	0.7	1.0
Eu	0.7	0.3	0.6	0.1	0.8	0.8	1.3	0.2	8.8	5.4	0.2	0.3
Gd	2.1	0.8	2.2	0.6	2.8	2.1	3.3	0.8	24.6	14.2	0.9	1.4
Tb	0.3	0.1	0.3	0.1	0.4	0.3	0.5	0.1	3.5	1.8	0.4	0.4
Dy	1.6	0.6	2.0	0.4	2.0	1.2	2.6	0.3	17.6	7.0	0.9	1.3
Ho	0.3	0.1	0.5	0.1	0.4	0.2	0.5	0.0	3.2	1.1	0.3	0.4
Er	0.9	0.3	1.4	0.2	1.1	0.5	1.5	0.1	8.4	2.7	0.6	0.9
Tm	0.1	0.0	0.2	0.0	0.1	0.1	0.2	0.0	1.0	0.3	0.1	0.1
Yb	0.7	0.2	1.1	0.2	0.8	0.3	1.7	0.1	5.6	1.9	0.5	0.5
Lu	0.1	0.0	0.2	0.0	0.1	0.0	0.3	0.0	0.8	0.3	0.2	0.2
ΣREE	64.6	16.6	64.4	7.5	105.4	50.6	161.0	47.5	937.3	713.7	16.8	15.8
Pr/Yb	1.4	0.2	0.7	0.1	1.9	0.4	1.2	0.3	2.4	1.1	0.5	0.3
Eu*	1.5	0.2	1.5	0.1	1.2	0.4	1.6	0.3	1.6	0.0	1.2	0.2
Ce*	1.0	0.3	0.8	0.3	1.1	0.2	1.6	0.3	0.9	0.0	0.9	0.4

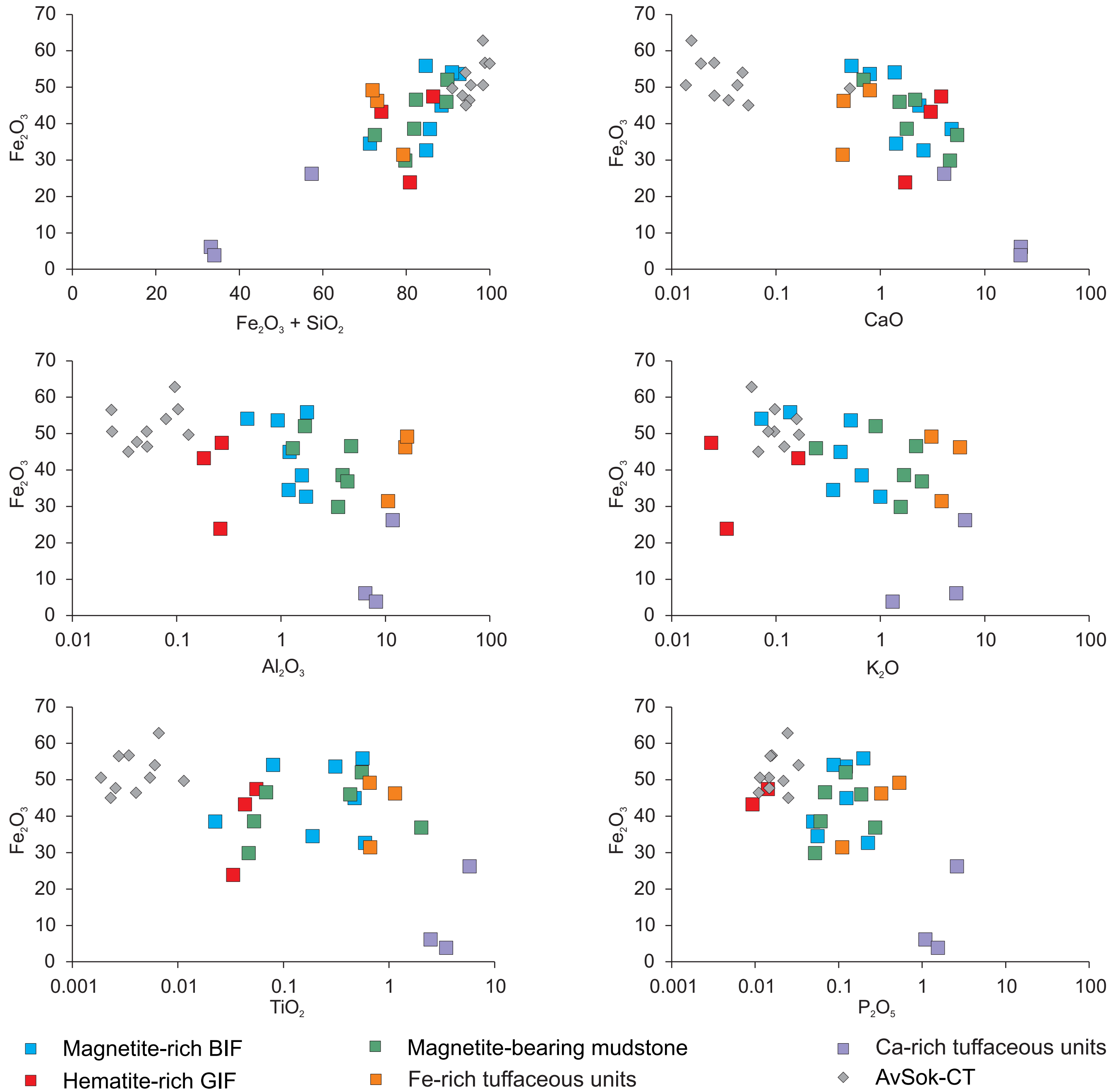

Figure 5. *Bivariate plots of Fe_2O_3* vs. *select major elements for samples of MBIF, HGIF, MM and Fe-rich and Ca-rich tuffaceous units. AvSok-CT = Average Sokoman Formation in the central Labrador Trough (from Conliffe, 2016).*

Hematite-rich Granular Iron Formation (HGIF)

The HGIF has similar $Fe_2O_3 + SiO_2$ contents to MBIF (80.5 ± 7 wt. %), with total Fe_2O_3 of 38.2 ± 12.6 wt. % (26.7 ± 8.78 wt. % Fe). The Al_2O_3, TiO_2, P_2O_5 and K_2O contents of the HGIF are generally lower than the MBIF, and are similar to AvSok-CT (Figure 5). However, HGIF contains significantly higher contents of MnO (4.8 to 14.3 wt. %) and has relatively high CaO contents.

The HGIF samples have very consistent trace-element concentrations, and with the exception of higher contents of Sr and Ba, they are similar to AvSok-CT (Figure 6).

The ∑REE content of HGIF samples ranges from 59 to 73 ppm, and compared to the MBIF they contain lower LREE contents (Pr/Yb_{PAASN} of 0.60 to 0.80). All samples have positive Eu anomalies (Eu/Eu^*_{PAASN} of 1.39 to 1.57).

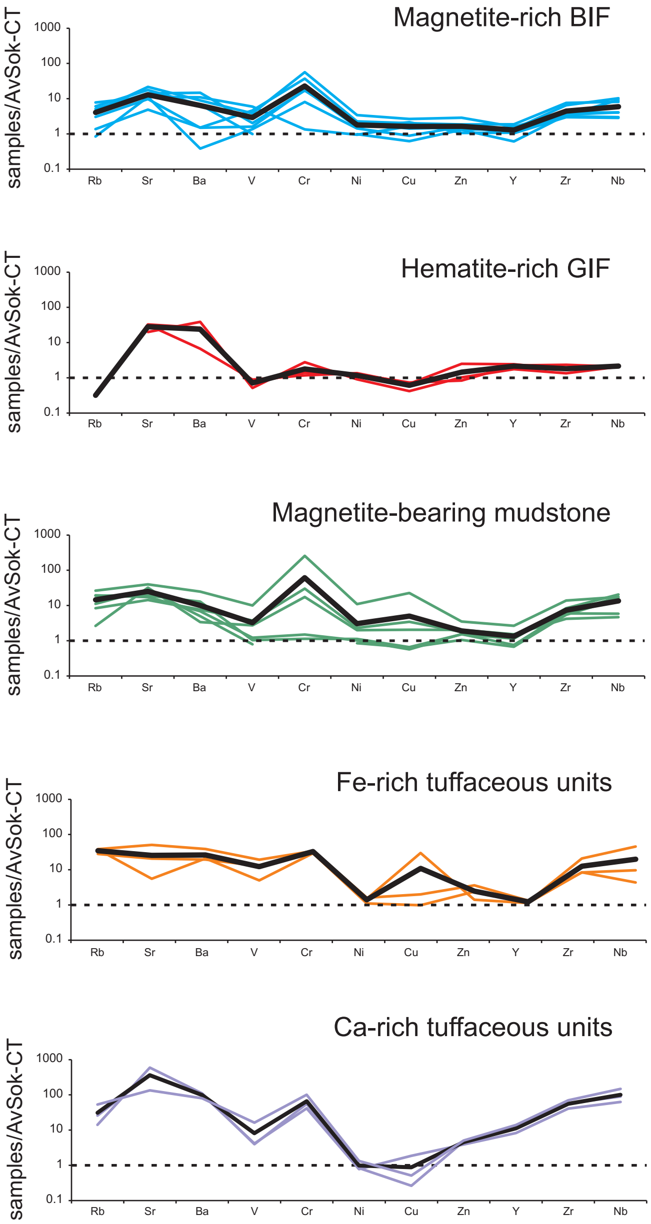

Figure 6. *Trace-element composition of MBIF, HGIF, MM and Fe-rich and Ca-rich tuffaceous units, normalized against AvSok-CT. Solid black line represents average of all samples.*

Magnetite-bearing Mudstone (MM)

The MM has total Fe_2O_3 + SiO_2 contents of 82.7 ± 6.5 wt. %, and Fe_2O_3 contents range from 29.8 to 52 wt. % (20.9 to 36.4 wt. % Fe). The CaO, TiO_2 and P_2O_5 contents of MM are similar to the MBIF, but it has relatively higher contents of Al_2O_3 and K_2O (Figure 5), and has a lower MnO contents (0.4 ± 0.2 wt. %).

The MM samples have variable trace-element contents (Figure 6). Three samples have very similar profiles as MBIF samples, with higher contents of LILE, Cr, Zr and Nb compared to AvSok-CT. In contrast, three other samples of MM have much lower trace-element contents, and do not show any enrichment in transition metals (including Cr).

Compared to AvSok-CT, all MM samples have strong to moderate increased contents of LREE (Pr/Yb_{PAASN} of 1.63 to 2.67; Figure 8) and have ∑REE ranging from 70 to 202 ppm. Three samples have positive Eu anomalies (Eu/Eu^*_{PAASN} of 1.49 to 1.56) and negligible Ce anomalies (Ce/Ce^*_{PAASN} of 0.88 to 0.94), which correspond with the higher contents of Cr. The samples that do not display increased contents of Cr have negative Eu anomalies (Eu/Eu^*_{PAASN} of 0.65 to 0.95) and weak to moderate positive Ce anomalies (Ce/Ce^*_{PAASN} of 1.11 to 1.32).

Fe-rich Tuffaceous Units

The Fe-rich tuffaceous units are defined based on their high Fe_2O_3 content (>30 wt. %) and low CaO content (<1 wt. %, Figure 5). The Fe_2O_3 + SiO_2 contents range from 71.9 to 79.3 wt. %, and they have higher Al_2O_3 (10.6 to 16.2 wt. %) and K_2O (3.1 to 5.5 wt. %) contents than MM and MBIF samples (Figure 5). The TiO_2 and P_2O_5 content of Fe-rich tuffaceous units are similar to MBIF and MM.

The trace-element profiles show that Fe-rich tuffaceous units have higher LILE, Zr and Nb contents when compared to AvSok-CT, and have variable transition metals contents (Figure 6).

The ∑REE content of Fe-rich tuffaceous units ranges from 108 to 200 ppm, and Figure 7 shows that they display slightly LREE enriched profiles (Pr/Yb_{PAASN} of 0.86 to 1.44). All samples show strong positive Eu anomalies (Eu/Eu^*_{PAASN} of 1.44 to 1.95), and also have positive Ce anomalies (Ce/Ce^*_{PAASN} of 1.29 to 1.87).

Ca-rich Tuffaceous Units

Ca-rich tuffaceous units have high CaO contents (4.1 to 22.2 wt. %), low Fe_2O_3 contents of 3.81 to 26.2 wt. % (Figure 5), and Al_2O_3 contents ranging from 6.4 to 11.8 wt. %. All other major elements have variable contents, but are generally higher than other rock types (Figure 5) with K_2O up to 6.5 wt. %, Na_2O up to 3.9 wt. %, TiO_2 up to 5.8 wt. %, MnO up to 5.8 wt. % and P_2O_5 up to 2.6 wt. %.

Figure 6 shows that Ca-rich tuffaceous units have much higher contents of LILE (Rb, Sr and Ba) and HFSE (Y, Zr and Nb) when compared to AvSok-CT. The relative concentrations of transition elements is more variable, with higher V and Cr contents, and similar Ni and Cu concentrations compared to AvSok-CT (Figure 6).

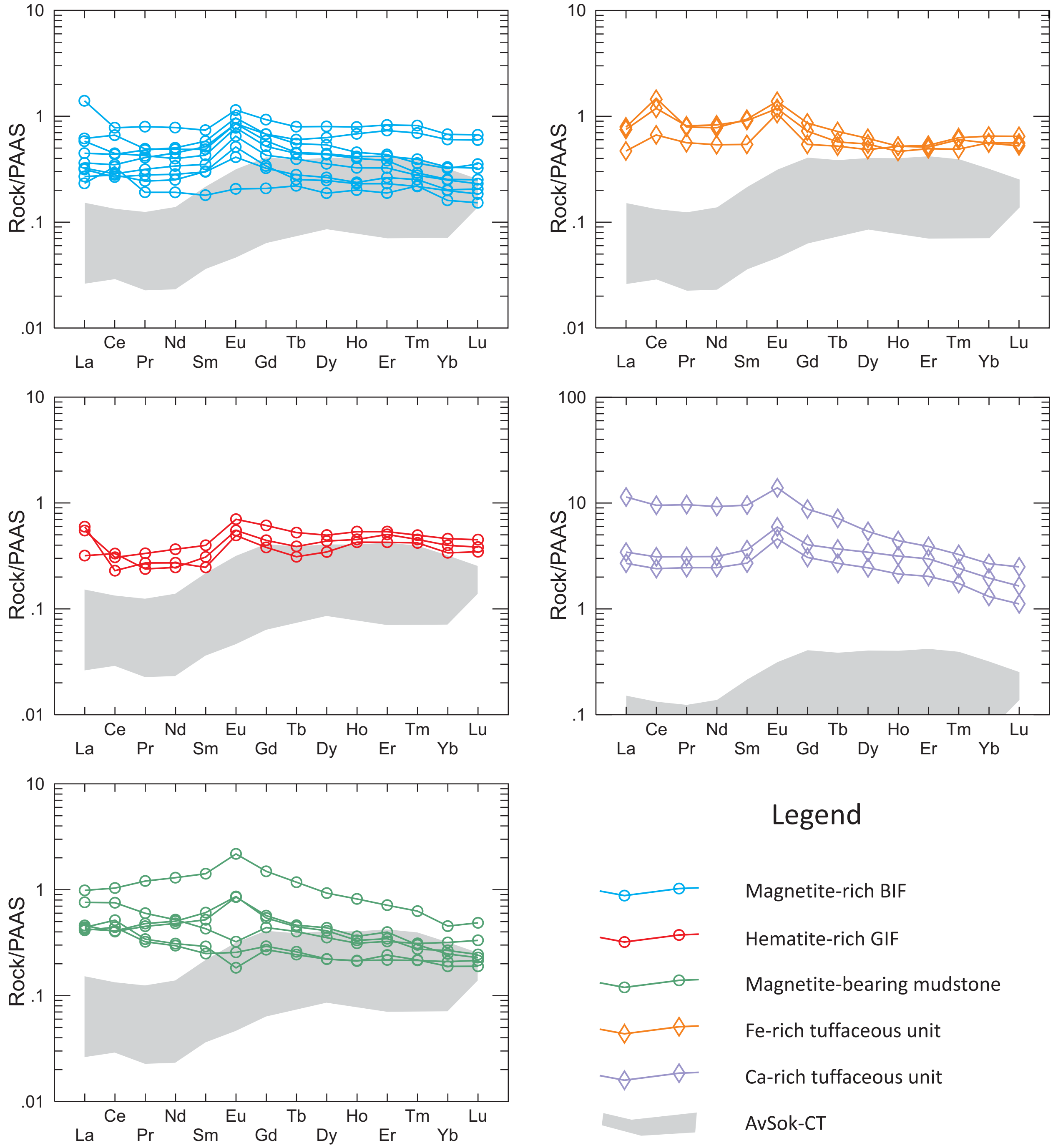

Figure 7. *REE distribution patterns normalized to Post-Archean (Average) Australian Shale (PAAS) for MBIF, HGIF, MM and Fe-rich and Ca-rich tuffaceous units. Shaded areas show the range of values for AvSok-CT (from Conliffe, 2016).*

Ca-rich tuffaceous units have high ∑REE contents, ranging from 460 to 1757 ppm, and are moderately to strongly enriched in LREE, with Pr/Yb_{PAASN} of 1.53 to 3.60 (Figure 8). All samples have positive Eu anomalies, with Eu/Eu^*_{PAASN} of 1.52 to 1.59, and negligible Ce anomalies (Ce/Ce^*_{PAASN} of 0.90 to 0.94).

DISCUSSION

New petrographic and lithogeochemical data from drill-core collected in the Gabbro Lake area provide information on the stratigraphy and depositional environment of the Sokoman and Wishart formations in the southeastern Labrador Trough.

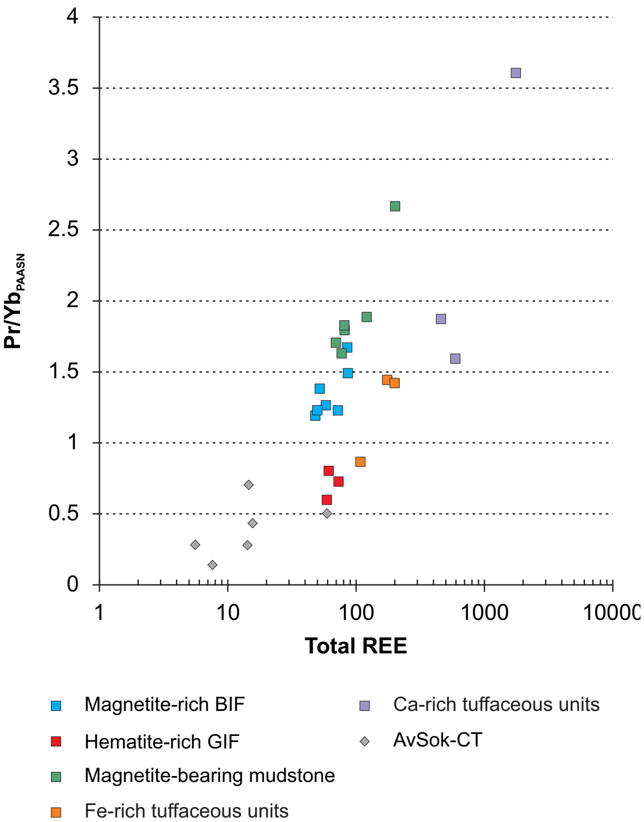

Figure 8. *Bivariate plot of* Pr/Yb_{PAASN} *against total REE content of MBIF, HGIF, MM and Fe-rich and Ca-rich tuffaceous units. AvSok-CT = Average Sokoman Formation in the central Labrador Trough (from Conliffe, 2016).*

Previous studies from the western margin of the Labrador Trough have shown that the Sokoman and Wishart formations were deposited on a dynamic paleoshelf on the margins of the Superior continent (Zajac, 1974; Simonson, 1984; Edwards *et al.*, 2012; Pufahl *et al.*, 2014). The Sokoman Formation in the Schefferville area is interpreted to represent two unconformity-bounded sequences that record the transition from lagoonal and supratidal environments to relatively deeper environments below the fair-weather wave base (Pufahl *et al.*, 2014). The presence of granular iron formation having abundant oolites, cross-stratified grainstones and rip-up clasts, and the occurrence of fossil bacteria, biofilms and stromatolites on the western margin of the Labrador Trough are all consistent with this interpretation of a shallow-water depositional environment (Zajac, 1974; Edwards *et al.*, 2012; Pufahl *et al.*, 2014).

The Sokoman Formation in the Gabbro Lake area is dominated by MBIF and fine-grained MM. The fine grain size and lamination of the MBIF and MM are consistent with deposition as a chemical mud in a low-energy environment, occurring either as direct precipitations from Fe-rich seawater as Fe-hydroxidal gels, or as hydrothermal muds deposited in a volcanic setting and re-sedimented by density currents, similar to that in the Red Sea (Krapež *et al.*, 2003; Bekker, 2010). These rocks likely precipitated in deep water below the storm wave base, in either an outer shelf or slope-break setting (Pufahl, 1996). The HGIF having well-developed oolitic textures and hematite > magnetite are restricted to thin (<5 m) units near the top of the Sokoman Formation. They are interpreted to have been deposited in a higher energy environment close to, or above, the storm wave base. The presence of GIF in the Sokoman Formation in the southeastern Labrador Trough could indicate that: 1) the depositional environment was above the storm wave base during periods of marine regression, or 2) that storm-generated turbidity currents originating in the nearshore environment transported shallow-marine, oolite-rich sediments out to the outer shelf environment (Pufahl, 1996).

The lateral facies variation from nearshore deposition of Sokoman Formation on the western margin of the Labrador Trough to the deposition in a deeper water, outer-shelf or slope environment in the southeastern Labrador Trough is similar to the pattern observed in Paleoproterozoic iron formations in the Lake Superior region (Pufahl, 1996). These facies variations have important implications for the metallurgy of taconite deposits, as well as the potential for upgrading of the iron formation to high-grade ore (>60% Fe) during hypogene and supergene processes (*see* below).

This study is the first to describe the presence of the Wishart Formation in the Gabbro Lake area, which was previously thought be absent in the southeastern Labrador Trough (Rivers, 1982; Noel, 1992). The Wishart Formation in the Schefferville area is dominated by fine- to coarse-grained sandstones with characteristics indicative of deposition in a high-energy, storm- to tide-dominated shelf environment (Simonson, 1984). In contrast, the Wishart Formation in the southeastern Labrador Trough is composed of an upper sequence of graded sandstones, conglomerates and quartz breccias that are underlain by black graphitic shales deposited in an outer shelf or continental slope setting. The black shales were likely deposited during a highstand, when the supply of clastic sediment was shut off as continental sediment was trapped in the nearshore environment (Arnott, 2010). The overlying conglomerates, breccias and sandstones may indicate rapid erosion of the nearshore sandstones during sea level fall, and these have a gradational contact with non-magnetic, iron-rich siltstones at the base of the overlying Sokoman Formation that reflect the onset of iron formation deposition.

The stratigraphy of the Kaniapiskau Supergroup below the Wishart Formation is similar to that recorded in the central Labrador Trough, with shales and siltstones of the Dolly

Formation, dolomitic limestones of the Denault Formation and shales of the Le Fer Formation all recorded in drillhole GL-12-02.

VOLCANIC ACTIVITY IN THE SOUTHEASTERN LABRADOR TROUGH

The presence of numerous tuffaceous units interbedded with the Sokoman Formation in the Gabbro Lake area indicates that there was significant volcanic activity in the southeastern Labrador Trough during deposition of the iron formation. All tuffaceous units contain fine-grained detrital material having <10% lithic fragments and phenocrysts. The obliteration of fine-scale primary textures by later deformation and metamorphism makes it difficult to determine if these units represent water-settled ash-fall tuffs or reworked volcaniclastic deposits. A reworked volcaniclastic origin is favoured, due to the wide range in composition (reflecting variable inputs from sedimentary and volcanic sources), the low abundance of volcanic detritus and the subrounded lithic fragments. Similar interpretations for the origins of tuffaceous units interbedded with the Sokoman Formation have been proposed elsewhere in the central and southeastern Labrador Trough (Rivers, 1982; Hassler and Simonson, 1989).

The Fe-rich tuffaceous units display strong chlorite alteration and were likely derived from basaltic material, possibly related to the Nimish volcanic centres occurring approximately 100 km to the northeast; an interpretation similar to that suggested for actinolite–chlorite schists interbedded with the Sokoman Formation from the McKay River area (Noel, 1992). The origin of the volcaniclastic detritus in the Ca-rich tuffaceous units is more enigmatic. They are devoid of basaltic detritus and are characterized by high CaO, TiO_2 and P_2O_5 (Figure 5) and commonly contain fragments of K-feldspar, quartz, albite and apatite. Therefore, it is unlikely that these tuffs are related to the Nimish volcanic centres. The source of the volcaniclastic material is probably from a volcanic centre to the east or south of the study area that was not preserved in the geological record. Noel (1992) recorded two distinct allochthonous volcanic sequences in the McKay River area, which were transported during the Grenville Orogeny. These include high CaO and TiO_2 basalts (McKay River Formation) and alkali ultrabasic lavas with affinities to olivine melilitite (Rose Bay Formation), and indicate the presence of a major volcanic centre to the south of the Gabbro Lake area at the time of deposition of the Sokoman Formation (Noel, 1992).

Whole-rock geochemistry combined with petrographic studies is useful in determining the source of detrital material in sedimentary rocks, including iron formations (Ewers and Morris, 1981; Horstmann and Hälbich, 1995; Zhang *et al.*, 2014). Iron formations typically have low Al_2O_3, K_2O, TiO_2 and trace-element contents (Klein and Beukes, 1992). Elevated concentrations of these elements in an iron formation are commonly related to detrital input, including volcaniclastic detritus (Ewers and Morris, 1981; Horstmann and Hälbich, 1995). In addition, the presence of stilpnomelane in iron formations is also a key indicator of volcanogenic provenance (Horstmann and Hälbich, 1995; Pickard, 2002; Krapež *et al.*, 2003).

The MBIF and MM are characterized by higher Al_2O_3, K_2O, TiO_2 and trace element than the HGIF or the AvSok-CT (Table 2; Figures 5 and 6), and the weakly metamorphosed MBIF and MM samples are rich in stilpnomelane. Al_2O_3 and TiO_2 are considered good indicators of clastic contamination, as they are unlikely to have precipitated directly from seawater and are commonly interpreted to be immobile during late-stage alteration and metamorphism (Ewers and Morris, 1981). Bivariate plots of Al_2O_3 and TiO_2 illustrate that five MBIF and three MM samples have relatively high TiO_2 and display a strong correlation with Ca-rich tuffaceous units ($R^2 = 0.97$; Figure 9), indicating a similar source of volcaniclastic detritus. Three MM and a single MBIF sample have a weaker correlation with Fe-rich tuffaceous units ($R^2 = 0.68$; Figure 9), which may be related to input of volcanoclastic detritus, or to a higher proportion of Al-rich clays in these samples.

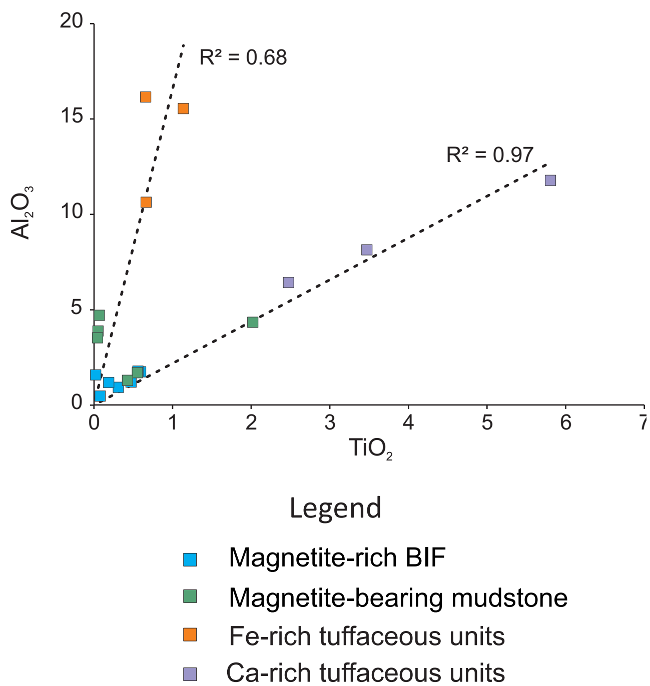

Figure 9. *Bivariate plot of Al_2O_3* vs. *TiO_2, with correlations between MBIF and MM samples with high TiO_2 and Ca-rich tuffaceous units, and MBIF and MM samples with lower TiO_2, which correlate with Fe-rich tuffaceous units.*

Other geochemical indicators show good correlations between all MBIF, MM and tuffaceous samples, such as Zr *vs.* TiO_2 ($R^2 = 0.89$), K_2O *vs.* Rb ($R^2 = 0.88$) and Nb *vs.* Ta ($R^2 = 0.90$), which are likely controlled by the relative abundance of detrital heavy minerals and volcaniclastic debris (Zhang *et al.*, 2014). The REE patterns show a similar linear trend, with increases in total REE corresponding to increase in Pr/Yb (Figure 8). The high REE totals and higher contents of LREE is in contrast to REE element content of the Sokoman Formation in the central Labrador Trough (AvSok-CT), and is unusual when compared to other iron formations worldwide (Derry and Jacobson, 1990). The higher concentrations are likely explained by an increase in percentage of LREE enriched detritus such as apatite (Belousova *et al.*, 2002).

ECONOMIC IMPLICATIONS

Diamond drilling in the Gabbro Lake area has intercepted up to 140 m of Sokoman Formation iron formation, and exploration farther to the north on Anomaly A (Figure 2) has intercepted 354 m of iron formation (@ 27.75% Fe; Froude and Fraser, 2013). Logging of drillcore has shown that these intercept thicknesses are associated with major synclinal structures and thrust repetition of the iron formation, likely having occurred during the Grenville Orogeny. Petrographic and geochemical studies have shown that the Sokoman Formation in the Gabbro Lake area is dominantly composed of a fine-grained banded iron formation, and significant amounts of Fe-silicates and relatively high Al_2O_3, TiO_2 and P_2O_5 compared to the Sokoman Formation on the western margin of the Labrador Trough. Therefore, metallurgical studies would be required to determine whether the Sokoman Formation in the Gabbro Lake area can produce an economic product.

ACKNOWLEDGMENTS

Alex Calon is thanked for his assistance during fieldwork, and Wayne Tuttle provided vital logistical support without which this project would be impossible. Tim Froude and Sokoman Iron Corp. are thanked for assistance during field visits, and with information on drilling programs. Chris Moran and the summer students of the Mines Branch drillcore storage program provided access to drillcore in Goose Bay, and aided in moving a large amount of core boxes. Sample preparation and geochemical analyses were carried out under the supervision of Chris Finch of the GSNL Geochemistry Laboratory. Gerry Kilfoil is thanked for helping to interpret geophysical data. I also extend my appreciation to Robert King, Dylan Goudie and David Grant (Memorial University of Newfoundland) for SEM-MLA sample preparation and data analysis. John Hinchey provided helpful reviews of early drafts of this contribution.

REFERENCES

Arnott, R.W.C.
2010: Deep-marine sediments and sedimentary systems. *In* Facies Models 4. *Edited by* N.P. James and R.W. Dalrymple. Geological Association of Canada, GEOtext 6, pages 295-322.

Baird, D.M.
1950: The geology of the Evening Lake-South Gabbro Lake area, southwestern Labrador. Newfoundland and Labrador Geological Survey, Assessment File 23H/0002, 59 pages.

Bekker, A., Slack, J.F., Planavsky, N., Krapez, B., Hofmann, A., Konhauser, K.O. and Rouxel, O.J.
2010: Iron formation; the sedimentary product of a complex interplay among mantle, tectonic, oceanic, and biospheric processes. Economic Geology, Volume 105, pages 467-508.

Beland, R.
1950: Report on the geology of the Gabbro Lake area, Labrador. Newfoundland and Labrador Geological Survey, Assessment File 23H/0003, 39 pages.

Belousova, E.A., Griffin, W.L., O'Reilly, S.Y., Fishera, N.I. and Breau, G.J.
2002: Apatite as an indicator mineral for mineral exploration: trace-element compositions and their relationship to host rock type. Journal of Geochemical Exploration, Volume 76, pages 45-69.

Breau, G.J.
1957: Geological anomaly investigation report of the Ossokmanuan Lake area, Labrador. Newfoundland and Labrador Geological Survey, Assessment File 23H/0010, 59 pages.

Brown, D.L.
1990: A structural analysis of the Grenville Front Zone, northeast Gagnon Terrane, Labrador. Unpublished M.Sc. thesis, Memorial University of Newfoundland, 190 pages.

Clark, T. and Wares, M.
2005: Lithotectonic and metallogenic synthesis of the New Québec Orogen (Labrador Trough). Ministère des Ressources naturelles, Québec, MM 2005-01, 175 pages.

Clout, J.M.F. and Simonson, B.M.
2005: Precambrian iron formations and iron formation-hosted iron ore deposits. Society of Economic Geologists, 100th Anniversary Volume, pages 643-679.

Conliffe, J.
2016: Geochemical data from high-grade iron-ore deposits and altered and unaltered iron formation in the Labrador Trough (NTS 23J and 23O). Government of Newfoundland and Labrador, Department of Natural Resources, Geological Survey, Open File LAB/1667, 35 pages.

Connelly, J.N. and Heaman, L.M.
1993: U–Pb geochronological constraints on the tectonic evolution of the Grenville Province, western Labrador. Precambrian Research, Volume 63, pages 123-142.

Derry, L.A. and Jacobsen, S.B.
1990: The chemical evolution of Precambrian seawater: evidence from REEs in banded iron formations. Geochimica et Cosmochimica Acta, Volume 54, pages 2965-2977.

Edwards, C.T., Pufahl, P.K., Hiatt, E.E. and Kyser, T.K.
2012: Paleoenvironmental and taphonomic controls on the occurrence of Paleoproterozoic microbial communities in the 1.88 Ga Ferriman Group, Labrador Trough, Canada. Precambrian Research, Volumes 212-213, pages 91-106.

Emslie, R.F., Hamilton, M.A. and Gower, C.F.
1997: The Michael Gabbro and other Mesoproterozoic lithospheric probes in southern and central Labrador. Canadian Journal of Earth Sciences, Volume 34, pages 1566-1580.

Evans, J.L.
1978: The geology and geochemistry of the Dyke Lake area (parts of 23J/8, 9), Labrador. Government of Newfoundland and Labrador, Department of Mines and Energy, Mineral Development Division, Report 78-04, 43 pages.

Ewers, W.E. and Morris, R.C.
1981: Studies of the Dales Gorge Member of the Brockman Iron Formation, Western Australia. Economic Geology, Volume 76, pages 1929-1953.

Findlay, J.M., Parrish, R.R., Birkett, T.C. and Watanabe, D.H.
1995: U–Pb ages from the Nimish Formation and Montagnais glomeroporphyritic gabbro of the central New Québec Orogen, Canada. Canadian Journal of Earth Sciences, Volume 32, pages 1208-1220.

Froude, T. and Fraser, D.
2012: First, second, fourth, fifth and sixth year assessment report on prospecting and geochemical and diamond drilling exploration for licences 13463M, 15510M, 17680M, 17683M, 18845M-18846M, 18882M, 19307M and 19910M-19911M on claims in the Gabbro Lake area, western Labrador, 2 reports. Newfoundland and Labrador Geological Survey, Assessment File 23H/0136, 105 pages.

2013: Report on Exploration Activities – 2013 Airborne Gravity Survey, Iron Horse Project, Labrador. Newfoundland and Labrador Geological Survey, Assessment File 023H/0150, 112 pages.

Fryer, J.J.
1977: Trace element geochemistry of the Sokoman Iron Formation. Canadian Journal of Earth Sciences, Volume 14, pages 1598-1610.

Gower, C.F., Rivers, T. and Brewer, T.S.
1990: Middle Proterozoic mafic magmatism in Labrador, eastern Canada. *In* Mid-Proterozoic Laurentia-Baltica. *Edited by* C.F. Gower, T. Rivers and A.B. Ryan. Geological Association of Canada, Special Paper 38, pages 485-506.

Grant, J.M.
1980: Report on an Airborne Geophysical Survey of block 124, Labrador. Newfoundland and Labrador Geological Survey, Assessment File 23H/11/0080, 5 pages.

Hassler, S.W. and Simonson, B.M.
1989: Deposition and alteration of volcaniclastic strata in two large, Early Proterozoic iron-formations in Canada. Canadian Journal of Earth Sciences, Volume 26(8), pages 1574-1585.

Horstmann, U.E. and Hälbich, I.W.
1995: Chemical composition of banded iron-formations of the Griqualand West Sequence, Northern Cape Province, South Africa, in comparison with other Precambrian iron formations. Precambrian Research, Volume 72(1), pages 109-145.

James, D.T.
1994: Geology of the Grenville Province in the Lac Joseph and Ossokmanuan Lake areas (23A/NW and 23H/SW), western Labrador. Government of Newfoundland and Labrador, Department of Mines and Energy, Geological Survey Branch, Report 94-02, 71 pages.

1995: Geology of the Paleoproterozoic Blueberry Lake group in the Gabbro Lake area, western Labrador. Map 95-004. Government of Newfoundland and Labrador, Department of Natural Resources, Geological Survey, Open File 23H/0102.

James D.T. and Connelly, J.N.
1995: Geology of the Paleoproterozoic Blueberry Lake Group, Grenville Province, western Labrador. *In* Current Research. Government of Newfoundland and Labrador, Department of Natural Resources, Geological Survey, Report 95-01, pages 25-36.

James, H.L.
1954: Sedimentary facies of iron-formation. Economic Geology, Volume 49, pages 235-293.

Klein, C. and Beukes, N.J.
1992: Time distribution, stratigraphy, sedimentologic setting, and geochemistry of Precambrian iron-formations. *In* The Proterozoic Biosphere, A Multidisciplinary Study. *Edited by* J.W. Schopf and C. Klein. New York, Cambridge University Press, pages 139-146.

Klein, C. and Bricker, O.P.
1977: Some aspects of the sedimentary and diagenetic environment of Proterozoic banded iron-formations. Economic Geology, Volume 72, pages 1457-1470.

Klein, C. and Fink, R.P.
1976: Petrology of the Sokoman Iron-Formation in the Howells River area, at the western edge of the Labrador Trough. Economic Geology, Volume 71, pages 453-487.

Krapež, B., Barley, M.E. and Pickard, A.L.
2003: Hydrothermal and resedimented origins of the precursor sediments to banded iron formations: Sedimentological evidence from the early Palaeoproterozoic Brockman Supersequence of Western Australia. Sedimentology, Volume 50, pages 979-1011.

Le Gallais, C.J. and Lavoie, S.
1982: Basin evolution of the Lower Proterozoic Kaniapiskau Supergroup, central Labrador Miogeocline (Trough), Québec. Bulletin of Canadian Petroleum Geology, Volume 30, pages 150-160.

Machado, N., Clark, T., David, J. and Goulet, N.
1997: U–Pb ages for magmatism and deformation in the New Québec Orogen. Canadian Journal of Earth Sciences, Volume 34, pages 716-723.

Noel, N. and Rivers, T.
1980: Geological mapping the Mckay River-Gabbro Lake area, western Labrador. *In* Current Research. Government of Newfoundland and Labrador, Department of Mines and Energy, Mineral Development Division, Report 80-01, pages 214-221.

Noel, N.T.
1992: The geology and geochemistry of the McKay River area volcanic rocks, western Labrador. Unpublished M.Sc. thesis, Memorial University of Newfoundland, 149 pages.

Peach, P.A.
1952: Geology of the South Gabbro Lake area, Labrador. Newfoundland and Labrador Geological Survey, Internal Report, Miscellaneous [023H/0006].

Pickard, A.L.
2002: SHRIMP U–Pb zircon ages of tuffaceous mudrocks in the Brockman Iron Formation of the Hamersley Range, Western Australia. Australian Journal of Earth Sciences, Volume 49, pages 491-507.

Pufahl, P.K.
1996: Stratigraphic architecture of a Paleoproterozoic iron formation depositional system: the Gunflint, Mesabi, and Cuyuna iron ranges. Unpublished M.Sc. thesis, Lakehead University, 167 pages.

Pufahl P.K., Anderson, S.L. and Hiatt E.E.
2014: Dynamic sedimentation of Paleoproterozoic continental margin iron formation, Labrador Trough, Canada: Paleoenvironments and sequence stratigraphy. Sedimentary Geology, Volume 309, pages 48-65.

Reid, W., Greenwood, R., Au, K., Legault, J. and Schein, E.
2009: First and second year assessment report on geophysical exploration for licences 13463M, 13465M, 13469M-13470M, 13474M-13475M, 13477M, 13488M, 13494M and 15510M on claims in the Gabbro Lake area, western Labrador, 2 reports. Newfoundland and Labrador Geological Survey, Assessment File 23H/0128, 71 pages.

Rivers, T.
1982: Preliminary report on the geology of the Gabbro Lake and Mckay River map areas (23H/11 and 23H/12), Labrador. Government of Newfoundland and Labrador, Department of Mines and Energy, Mineral Development Division, Report 82-02, 30 pages.

Rivers, T., Culshaw, N., Hynes, A., Indares, A., Jamieson, R. and Martignole, J.
2012: The Grenville Orogen–a post-lithoprobe perspective. *In* Tectonic Styles in Canada: The Lithoprobe Perspective. *Edited by* F. Cook, J. Percival and R. Clowes.

Geological Association of Canada, Special Paper 49, pages 97-236.

Rohon, M.-L., Vialette, Y., Clark, T., Roger, G., Ohnenstetter, D. and Vidal, P.
1993: Aphebian mafic–ultramafic magmatism in the Labrador Trough (New Québec): its age and the nature of its mantle source. Canadian Journal of Earth Sciences, Volume 30, pages 1582-1593.

Simonson, B.M.
1984: High energy shelf-deposit; early Proterozoic Wishart Formation, northeastern Canada. Special Publication – Society of Economic Paleontologists and Mineralogists, Volume 34, pages 251-268.

Slipp, R.M.
1952: Geological report of the Margo Bay, Cavers Lake, Dodette Lake, Point Lake and Gabbro Lake areas, Labrador. Newfoundland and Labrador Geological Survey, Assessment File 23J/0017, 32 pages.

Sylvester, P.J.
2012: Use of the mineral liberation analyzer (MLA) for mineralogical studies of sediments and sedimentary rocks. Mineralogical Association of Canada, Short Course 42, pages 1-16.

Tiphane, M.
1951: Geology of the Tiphane Lake area, Labrador. Newfoundland and Labrador Geological Survey, Assessment File 23H/0018, 10 pages.

Wardle, R.J.
1979a: Geology of the southeastern Labrador Trough. In Report of Activities. Government of Newfoundland and Labrador, Department of Mines and Energy, Mineral Development Division, Report 79-01, pages 115-121.

1979b: Geology of the eastern margin of the Labrador Trough. Government of Newfoundland and Labrador, Department of Mines and Energy, Mineral Development Division, Report 78-09, 27 pages.

Wardle, R.J. and Bailey, D.G.
1981: Early Proterozoic sequences in Labrador. *In* Proterozoic Basins of Canada. *Edited by* F.H.A. Campbell. Geological Survey of Canada, Paper 81-10, pages 331-359.

Wardle, R.J., James, D.T., Scott, D.J. and Hall, J.
2002: The Southeastern Churchill Province: synthesis of a Paleoproterozoic transpressional orogen: Proterozoic evolution of the northeastern Canadian Shield: Lithoprobe Eastern Canadian Shield onshore–offshore transect. Canadian Journal of Earth Sciences, Volume 39, pages 639-663.

Wardle, R.J., Ware, M.J., Noel, N., Rivers, T. and Britton, J.M.
1985: Geology of the Gabbro Lake area, Labrador. Government of Newfoundland and Labrador, Department of Mines and Energy, Mineral Development Division, Map 85-026.

Ware, M.J. and Wardle, R.J.
1979: Geology of the Sims-Evening Lake area, western Labrador with emphasis on the Helikian Sims Group. Government of Newfoundland and Labrador, Department of Mines and Energy, Mineral Development Division, Report 79-05, 27 pages.

Wynne-Edwards, H.R.
1961: Ossokmanuan Lake, west half, Newfoundland. Geological Survey of Canada, preliminary map 17-1961.

Zajac, I.S.
1974: The stratigraphy and mineralogy of the Sokoman Iron Formation in the Knob Lake area, Québec and Newfoundland. Geological Survey of Canada, Bulletin 220, 159 pages.

Zhang, Y., Pe-Piper, G. and Piper, D.J.W.
2014: Sediment geochemistry as a provenance indicator: Unravelling the cryptic signatures of polycyclic sources, climate change, tectonism and volcanism. Sedimentology, Volume 61, pages 383-410.